EARTHQUAKE ENGINEERING AND STRUCTURAL DYNAMICS
Earthquake Engng Struct. Dyn. 2007; **36**:1275–1301
Published online 27 February 2007 in Wiley InterScience (www.interscience.wiley.com). DOI: 10.1002/eqe.679

Prediction of elastic displacement response spectra in Europe and the Middle East

Sinan Akkar[1,*,†] and Julian J. Bommer[2]

[1]*Earthquake Engineering Research Centre, Department of Civil Engineering, Middle East Technical University, 06531 Ankara, Turkey*
[2]*Department of Civil & Environmental Engineering, Imperial College London, London SW7 2AZ, U.K.*

SUMMARY

Empirical equations are presented for the prediction of displacement response ordinates for damping ratios of 2, 5, 10, 20 and 30% of critical and for response periods up to 4 s, using 532 accelerograms from the strong-motion databank from Europe and the Middle East. The records were all re-processed and only employed for regressions at periods within the usable range, defined as a fraction of the filter cut-off and depending on the instrument type (digital or analogue), earthquake magnitude and site class. The equations can be applied to predict the geometric mean displacement and pseudo-acceleration spectra for earthquakes with moment magnitudes (**M**) between 5 and 7.6, and for distances up to 100 km. The equations also include style-of-faulting and site class as explanatory variables. The predictions obtained from these new equations suggest that earlier European equations for spectral displacements underestimate the ordinates at longer periods as a result of severe filtering and the use of the spectral ordinates at periods too close to the filter cut-off. The results also confirm that the period defining the start of the constant displacement plateau in the Eurocode 8 (EC8) spectrum is excessively short at 2 s. The results not only show that the scaling factor defined in EC8 for estimating the spectral ordinates at damping ratios different from 5% of critical are a good general approximation, but also that this scaling varies with magnitude and distance (reflecting the influence of duration) and also displays a mild dependence on response period.

Received 10 September 2006; Revised 16 December 2006; Accepted 24 December 2006

KEY WORDS: displacement response spectra; pseudo-acceleration spectra; ground-motion prediction equations; European strong-motion database; Eurocode 8; displacement-based design; damping ratios

1. INTRODUCTION

Advances in earthquake-resistant design approaches inevitably create new requirements in terms of the definition of seismic actions. The increasing use of base isolation and supplementary damping

*Correspondence to: Sinan Akkar, Earthquake Engineering Research Centre, Department of Civil Engineering, Middle East Technical University, 06531 Ankara, Turkey.
†E-mail: sakkar@metu.edu.tr

devices to enhance seismic performance gives rise to the need for elastic design response spectra that extend to longer periods than have traditionally been considered, and also have higher damping ratios than the nominal 5% of critical assumed in most design codes.

The same long-period and highly-damped response spectral ordinates are also required for direct displacement-based design approaches that make use of equivalent linearization (e.g. [1]). Some researchers have shown that the use of equivalent linearization in displacement-based design may result in biased deformation demand estimations particularly for weak structures (e.g. [2]). However, both FEMA-440 [3] and Eurocode 8 (EC8) [4] acknowledge the viability of both equivalent linear and displacement modification approaches, given that each has its own advantages and limitations, and a consensus view has yet to be reached amongst earthquake engineers. Although EC8 does envisage, through Informative Annexes, the possible use of both approaches to displacement-based design, the implementation of the equivalent linearization approach is currently far less developed in the code [5].

One of the primary motivations for the present study is precisely to provide predictive equations for displacement response ordinates that may be used to re-evaluate the spectra currently defined in EC8. Concern has been expressed recently that the EC8 spectral ordinates may be excessively low at longer periods [5, 6], particularly if compared with those defined for the U.S. in NEHRP 2003 [7]. In the latter code, the constant displacement plateau begins at periods ranging from 4 to 16 s, whereas the EC8 Type 1 spectrum (for the higher seismicity regions of Europe) has a constant displacement plateau commencing at just 2 s. Ground-motion prediction equations in Europe have generally been limited to rather short response periods, as a result of the regional databank being composed primarily of analogue recordings and the usable period range, which is somewhat less than the filter cut-off period, of such accelerograms being limited (e.g. [8]). Ambraseys *et al.* [9] limited their predictions of spectral accelerations to 2 s, and Ambraseys *et al.* [10] subsequently extended the range to 2.5 s. The European equations of Berge-Thierry *et al.* [11], on the other hand, provide coefficients for response periods up to 10 s, but the records from which these were obtained were filtered at 4 s.

Of course the same results could be obtained by deriving equations for pseudo-acceleration response ordinates which can then be transformed to displacements. However, since the applications for which this work is aimed often use displacements directly, we have opted to define the response in terms of spectral displacements. Another reason for this choice is the fact that the next stage of this work is the derivation of equations for the prediction of inelastic displacement response and therefore this will permit easier comparisons than infer reduction factors and their dependence on seismological parameters. It should be noted that the elastic spectral displacements estimated from the predictive equations presented are equivalent to pseudo-acceleration ordinate predictions through the relationship between spectral displacement and pseudo-spectral acceleration.

The displacement spectrum defined in the current edition of EC8 (Figure 1) was based on work by Tolis and Faccioli [12] and Bommer and Elnashai [13], the former employing mainly digital accelerograms from the 1995 Kobe earthquake and the latter a databank of almost exclusively analogue accelerograms from Europe and the Middle East. Bommer and Elnashai [13] only produced coefficients for response periods up to 3 s, but the records may have been rather severely filtered and moreover spectral ordinates from each record were used up to 0.1 s less than the filter-cut off, where the response is strongly affected by the filter. The consequence of the stringent filters applied and the use of ordinates at periods so close to the filter cut-off was almost definitely to have underestimated the spectral displacements at intermediate- and long-periods.

DOI: 10.1002/eqe

Faccioli *et al*. [14] investigated long-period spectral ordinates using digital recordings of various earthquakes from Japan, Italy, Greece and Taiwan. They note in their study that for the **M**7.6 Chi Chi earthquake, the displacement spectra of near-source recordings have a plateau starting beyond 10 s, although for the **M**6.9 Kobe earthquake and recordings from moderate events, obtained by K-Net and European networks, the displacement plateau was found to start at periods of 2 s or less. Faccioli *et al*. [14] concluded that 'the dependence on magnitude of the T_D control period defining the beginning of the plateau of the elastic displacement spectrum should be carefully considered, especially for large magnitude earthquakes'. Bommer and Elnashai [13] had noted a weak dependence of the corner period on magnitude (and also site class), increasing in their formulation from 2.0 s at M_S 5.5 to 3.0 s for M_S 7.5, on rock, and from 2.7 s at M_S 5.5 to greater than 3.0 s at M_S 7.0 on soft soil. These results are compatible with source corner period that shifts to longer spectral periods with increasing magnitude. However, these findings were overlooked in the derivation of EC8, which adopted a constant value of 2.0 s for the Type 1 spectrum on all site classes, despite the fact that this does not conform with seismological theory which suggests that this control period should vary in inverse proportion to the corner frequency.

As well as attempting to obtain more robust estimates of the displacement response ordinates at intermediate periods using the European strong-motion databank, the present study also aims to provide information for an improved estimate of the spectral ordinates at damping values different from 5% of critical. EC8 enables spectral ordinates at higher damping values to be estimated by applying the following scaling factor to the 5%-damped ordinates:

$$\frac{\mathrm{SD}(\xi)}{\mathrm{SD}(5\%)} = \sqrt{\frac{10}{5+\xi}} \tag{1}$$

The scaling factor is applied between control periods T_B and T_E (Figure 1) and is linearly interpolated to 1.0 at periods of zero and T_F. Equation (1) was taken from Bommer *et al*. [15] and replaced a different equation that appeared in the first version of EC8 [16]. Tolis and Faccioli [12] also proposed a scaling factor, which differs from both the EC8 formulae, prompting an exploration of why these scaling factors, and those encountered in other seismic design codes, show such marked variation. Part of the reason for the lack of agreement amongst the various scaling factors is that they are generally independent of period in the range of the plateaus of constant acceleration, velocity and displacement, and the values will therefore depend on the shape of the spectra used for their derivation and the period ranges considered for calculating representative values. Bommer and Mendis [17] also found that the ratio of displacement ordinates at different damping values displays a marked dependence on the duration of the ground motion. Mendis and Bommer [18] derived duration-dependent scaling factors but note that these are not suitable for design code implementation since ground-motion duration is not presented in the codes. In the case of EC8, with separate spectral shapes for regions of high and low seismicity, adjustments could be made to the scaling factors to account for the duration of motion associated with different magnitude earthquakes [19]. However, the spectral shapes employed in EC8, both anchored only to peak ground acceleration (PGA), provide a very crude approximation of the uniform hazard spectrum and the formulation of seismic actions should be overhauled in future revisions of the code [5].

DOI: 10.1002/eqe

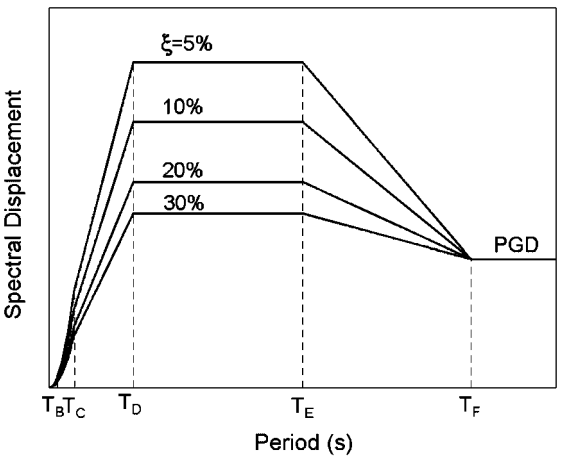

Figure 1. Displacement response spectra from Eurocode 8 on linear axes. The periods T_B and T_C correspond to the lower and upper limits of constant acceleration plateau whereas T_D and T_E are the controlling periods for constant displacement plateau. The period T_F indicates where the spectral displacements reach peak ground displacement (PGD). These control periods are defined for the Type 1 and Type 2 spectra as a function of site class.

2. DATA SET AND REGRESSION ANALYSES

The data set used for this study is the same as that recently employed by Akkar and Bommer [20] to derive predictive equations for peak ground velocity (PGV). The database is essentially that used by Ambraseys *et al.* [10], but the records were systematically re-filtered by Akkar and Bommer [21]. The data set contains a total of 532 accelerograms from 131 earthquakes of moment magnitude from 5.0 to 7.6. The details of the data set and the distribution with respect to magnitude, style-of-faulting, distance and site classification are presented together with the PGV prediction equations of Akkar and Bommer [20] and are not repeated here in order to save space.

Akkar and Bommer [21] established criteria for the maximum usable response period for the calculation of elastic displacement response spectra from filtered accelerograms. Applying these criteria to the data set means that as the response period increases fewer records are available for the regression analysis (Figure 2), although it is clear that the loss of usable data with increasing response period is, as would be expected, far more rapid for analogue than for digital data. Figure 3 shows the magnitude-distance-site class distribution of the records retained at different response periods.

From Figure 2 it can be appreciated that some rock analogue recordings become unusable even at periods as short as a little over 1 s, whereas for digital accelerograms the loss of data begins at around 3 s. There is an abrupt and significant loss of data at around 3.25 s, for both types of recordings. On the basis of the distributions shown in Figure 3, it was judged that at periods beyond 4 s the data would be insufficient to allow robust regression analyses and this was therefore selected as the limiting period. For a few digital recordings from larger earthquakes, the usable period range is considerable, and these could be used to guide extrapolation of the spectral ordinates to longer

DOI: 10.1002/eqe

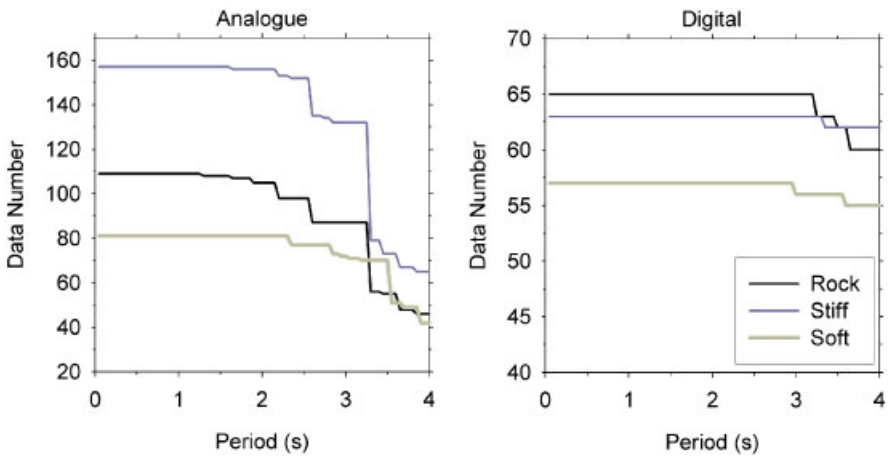

Figure 2. Period-dependent variation of usable data in terms of recording type and site conditions.

periods. However, for this study we have focused on deriving robust equations for the spectral displacements up to 4 s.

The functional form selected for the equation is the same as that used by Akkar and Bommer [20] for the prediction of PGV, and the reader is referred to that paper for a detailed discussion of this choice. The equation that predicts the geometric mean spectral displacement has the following form:

$$\log[\mathrm{SD}(T,\xi)] = b_1 + b_2\mathbf{M} + b_3\mathbf{M}^2 + (b_4 + b_5\mathbf{M})\log\sqrt{R_{\mathrm{jb}}^2 + b_6^2} + b_7 S_S + b_8 S_A + b_9 F_{\mathrm{N}} + b_{10} F_{\mathrm{R}} \quad (2)$$

where $\mathbf{M}$ is moment magnitude, R_{jb} is the Joyner–Boore distance in kilometres, S_S and S_A are binary variables taking values of 1 for soft and stiff soil sites, respectively (and zero otherwise), and F_N and F_R are similarly derived for normal and reverse faulting earthquakes.

The coefficients b_1–b_{10} were estimated using a maximum likelihood one-stage regression, as described in Akkar and Bommer [20]. The regressions consider inter- and intra-event variability separately, and pure error analysis, as used by Ambraseys *et al*. [10], was employed to determine the magnitude dependence of these variabilities. Again, the reader is referred to Akkar and Bommer [20] for more details.

The response spectra obtained from the equations were found to be jagged in appearance, particularly at longer periods for which in effect different data were used for each regression because of the limits imposed by the filter cut-offs. Therefore, it was decided to apply negative exponential smoothing [22] for each regression coefficient against period. Figure 4 shows the smoothing for coefficients b_1–b_6 for the 2%-damped spectral ordinates; the smoothing was also applied to the other four coefficients, but the resulting spectra are most sensitive to those controlling the dependence on magnitude and distance. Smoothing was also attempted with low-order polynomials, in the hope of achieving very smooth spectra, but as a result of the complex functional

DOI: 10.1002/eqe

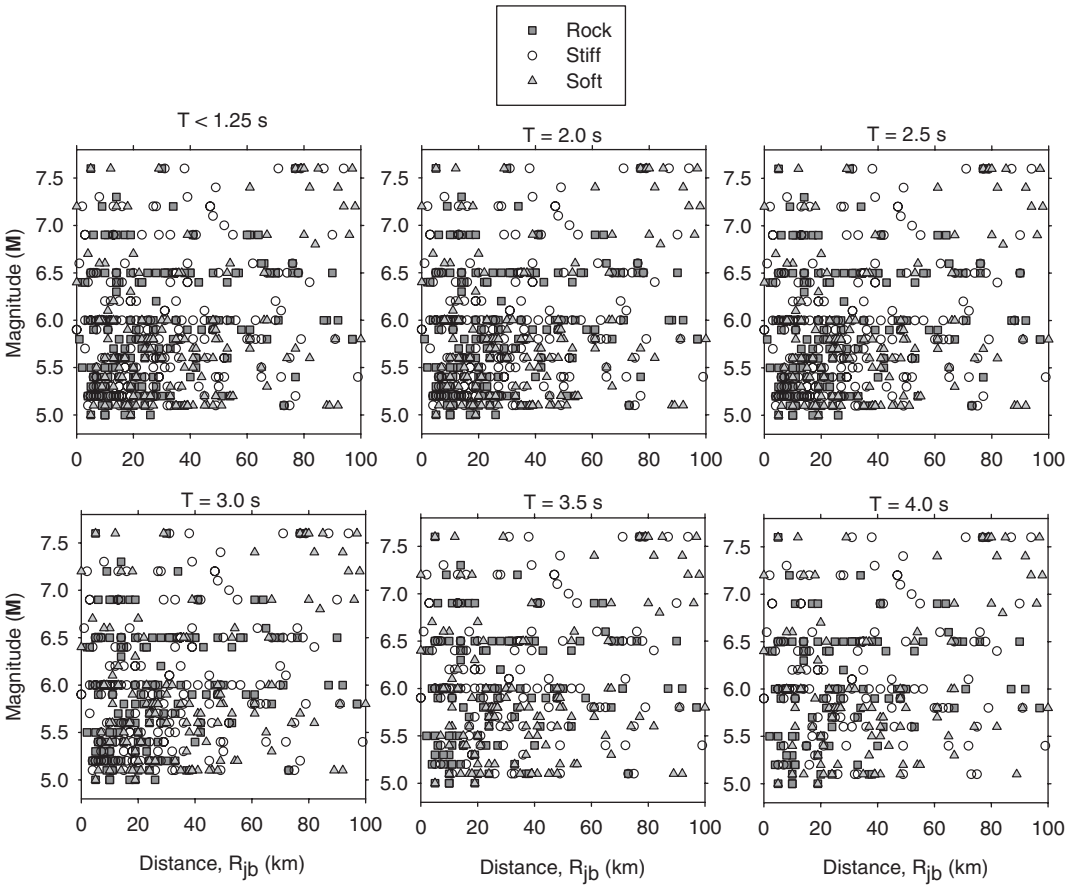

Figure 3. Magnitude-distance-site class distribution of database at different periods.

form the predictions were found to be excessively sensitive to trade-offs amongst the smoothed coefficients.

The smoothed regression coefficients b_1–b_6 are presented in Tables I–V for the five damping ratios considered. It was found that coefficients for site class and style-of-faulting dependence were very similar for different damping ratios, which is consistent with the duration dependence identified by Bommer and Mendis [17], since duration is only weakly influenced by site class and is almost independent of style-of-faulting. For this reason, in order to simplify the presentation and implementation of the results, the smoothed regression coefficients b_7–b_{10} are presented separately in Table VI as three sets that account for the damping ratios of 2 and 5%, 10 and 20% and 30%, respectively. Note that b_9 is virtually the same for all damping values, whereas b_7 and b_8 show differences only in the short spectral period range ($T \leqslant 0.45$ s) and the coefficient b_{10} differs for $T \geqslant 2.90$ s. The standard deviations, for both the inter- and intra-event components of the variability, calculated using the smoothed regression coefficients, are presented in Tables I–V.

DOI: 10.1002/eqe

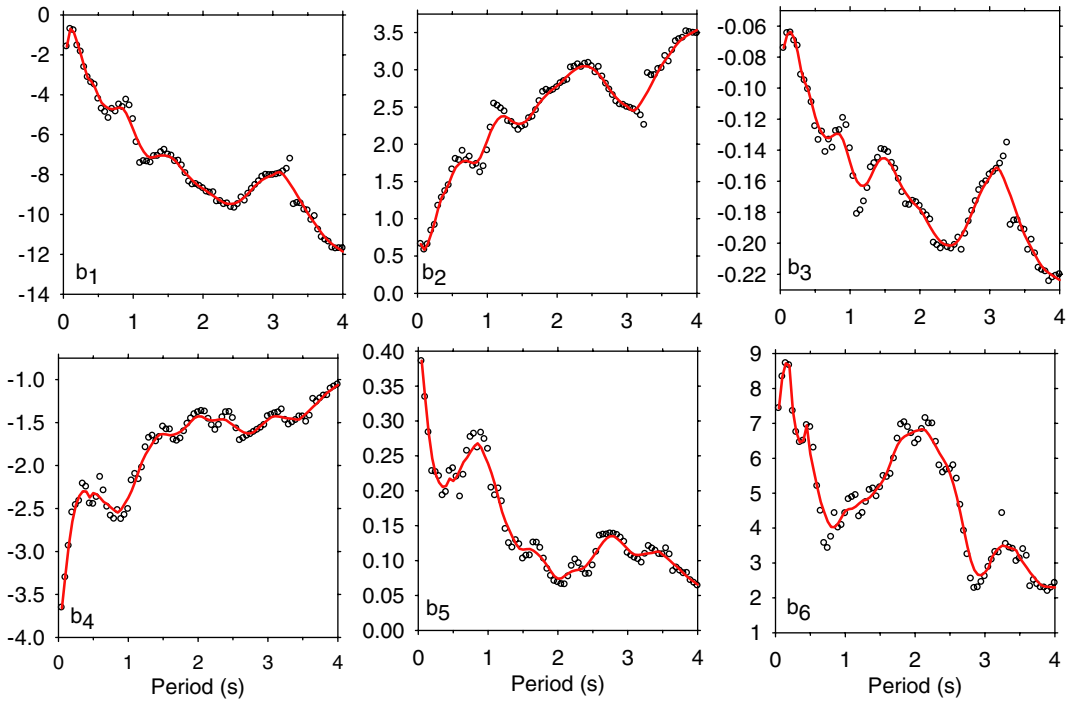

Figure 4. Illustrative example for the comparison of raw and smoothed regression coefficients b_1–b_6 for 2%-damped spectral ordinates.

Whereas it may have been expected to encounter slightly reduced variability for higher damping ratios, by virtue of the smoothing effect of the increased viscous damping, the variability shows no marked variation with damping level.

Figure 5 compares the spectrum obtained for a single earthquake scenario using the raw and smoothed coefficients. In order to show the compatibility of the smoothed coefficients with the variation in pseudo-spectral acceleration, the panel on the right compares the raw and smoothed PSA ordinates computed from the predicted SD. At periods close to 3 s and above, there are fluctuations in the predicted displacement spectra, especially for low damping ratios, which are a result primarily of the sharp decrease in usable data in this period range.

3. PREDICTIVE EQUATIONS FOR SPECTRAL DISPLACEMENT

Figure 6 compares the predictions of displacement spectra on rock sites using the equations of Bommer *et al.* [23] and the new equations presented here. Adjustments have been made to magnitudes and horizontal components of motion to correct for different definitions employed in the equations [24, 25]. The predictive equation of Bommer *et al.* [23] is independent of style-of-faulting but this does not introduce bias to the comparisons. In all the plots it is apparent that the new equations do not indicate a significant systematic difference in the spectral

DOI: 10.1002/eqe

Table I. Regression coefficients b_1–b_6 for 2%-damped spectral ordinates (σ_1 and σ_2 denote the intra- and inter-event standard deviations, respectively).

Period (s)	b_1	b_2	b_3	b_4	b_5	b_6	σ_1	σ_2
0.05	−1.592	0.660	−0.074	−3.661	0.386	7.431	0.536-0.043**M**	0.220-0.018**M**
0.10	−0.696	0.584	−0.065	−3.286	0.332	8.334	0.591-0.052**M**	0.247-0.022**M**
0.15	−0.863	0.664	−0.064	−2.935	0.283	8.718	0.534-0.042**M**	0.232-0.018**M**
0.20	−1.407	0.807	−0.068	−2.653	0.246	8.660	0.414-0.022**M**	0.156-0.008**M**
0.25	−1.966	0.963	−0.077	−2.460	0.223	7.351	0.595-0.051**M**	0.193-0.016**M**
0.30	−2.581	1.145	−0.089	−2.355	0.212	6.747	0.626-0.055**M**	0.170-0.015**M**
0.35	−3.162	1.294	−0.096	−2.299	0.205	6.456	0.611-0.052**M**	0.174-0.015**M**
0.40	−3.327	1.362	−0.101	−2.304	0.207	6.500	0.614-0.052**M**	0.206-0.018**M**
0.45	−3.621	1.469	−0.110	−2.371	0.217	6.944	0.745-0.073**M**	0.244-0.024**M**
0.50	−4.054	1.593	−0.119	−2.321	0.214	6.120	0.886-0.093**M**	0.261-0.027**M**
0.55	−4.407	1.689	−0.125	−2.336	0.220	5.649	0.861-0.090**M**	0.287-0.030**M**
0.60	−4.576	1.740	−0.129	−2.378	0.230	5.167	0.921-0.100**M**	0.346-0.038**M**
0.65	−4.686	1.772	−0.132	−2.424	0.241	4.746	0.997-0.112**M**	0.390-0.044**M**
0.70	−4.727	1.780	−0.132	−2.449	0.248	4.453	1.159-0.137**M**	0.460-0.054**M**
0.75	−4.691	1.763	−0.131	−2.487	0.256	4.189	1.394-0.170**M**	0.473-0.058**M**
0.80	−4.644	1.747	−0.129	−2.520	0.263	4.034	1.712-0.215**M**	0.459-0.058**M**
0.85	−4.685	1.756	−0.130	−2.548	0.268	4.030	1.573-0.197**M**	0.463-0.058**M**
0.90	−4.922	1.821	−0.133	−2.511	0.262	4.143	1.618-0.202**M**	0.486-0.061**M**
0.95	−5.306	1.929	−0.140	−2.444	0.250	4.316	1.513-0.188**M**	0.459-0.057**M**
1.00	−5.742	2.052	−0.148	−2.377	0.239	4.491	1.369-0.168**M**	0.464-0.057**M**
1.05	−6.168	2.169	−0.155	−2.293	0.225	4.545	1.152-0.137**M**	0.457-0.055**M**
1.10	−6.551	2.266	−0.160	−2.187	0.208	4.556	1.017-0.117**M**	0.403-0.046**M**
1.15	−6.860	2.336	−0.163	−2.067	0.189	4.616	0.998-0.114**M**	0.406-0.047**M**
1.20	−7.069	2.375	−0.163	−1.955	0.170	4.707	0.955-0.108**M**	0.401-0.045**M**
1.25	−7.152	2.378	−0.161	−1.869	0.155	4.785	0.834-0.089**M**	0.374-0.040**M**
1.30	−7.130	2.351	−0.157	−1.804	0.145	4.815	0.794-0.083**M**	0.350-0.037**M**
1.35	−7.070	2.312	−0.152	−1.737	0.134	4.878	0.814-0.086**M**	0.361-0.038**M**
1.40	−7.040	2.284	−0.148	−1.679	0.124	4.986	0.829-0.089**M**	0.376-0.040**M**
1.45	−7.044	2.273	−0.145	−1.639	0.117	5.117	0.836-0.091**M**	0.383-0.041**M**
1.50	−7.078	2.280	−0.145	−1.634	0.116	5.240	0.816-0.087**M**	0.370-0.040**M**
1.55	−7.155	2.306	−0.147	−1.641	0.116	5.395	0.892-0.099**M**	0.377-0.042**M**
1.60	−7.299	2.355	−0.150	−1.649	0.117	5.607	0.890-0.099**M**	0.388-0.043**M**
1.65	−7.507	2.422	−0.155	−1.643	0.114	5.875	0.913-0.103**M**	0.423-0.048**M**
1.70	−7.730	2.494	−0.160	−1.627	0.110	6.155	0.892-0.099**M**	0.429-0.048**M**
1.75	−7.939	2.559	−0.164	−1.605	0.106	6.383	0.849-0.092**M**	0.423-0.046**M**
1.80	−8.123	2.614	−0.168	−1.571	0.099	6.540	0.768-0.079**M**	0.395-0.040**M**
1.85	−8.298	2.664	−0.171	−1.532	0.092	6.624	0.765-0.078**M**	0.403-0.041**M**
1.90	−8.465	2.710	−0.174	−1.487	0.084	6.679	0.757-0.077**M**	0.412-0.042**M**
1.95	−8.598	2.747	−0.176	−1.447	0.078	6.726	0.708-0.069**M**	0.397-0.039**M**
2.00	−8.714	2.783	−0.178	−1.427	0.074	6.781	0.738-0.074**M**	0.417-0.042**M**
2.05	−8.829	2.824	−0.182	−1.430	0.075	6.804	0.687-0.066**M**	0.392-0.038**M**
2.10	−8.956	2.873	−0.186	−1.450	0.078	6.833	0.646-0.059**M**	0.365-0.033**M**
2.15	−9.078	2.919	−0.190	−1.469	0.082	6.799	0.657-0.061**M**	0.365-0.034**M**
2.20	−9.196	2.960	−0.193	−1.477	0.085	6.668	0.708-0.069**M**	0.394-0.038**M**
2.25	−9.310	2.997	−0.197	−1.473	0.086	6.502	0.695-0.067**M**	0.393-0.038**M**
2.30	−9.413	3.028	−0.199	−1.465	0.087	6.326	0.731-0.073**M**	0.419-0.042**M**
2.35	−9.467	3.044	−0.201	−1.462	0.088	6.142	0.787-0.082**M**	0.445-0.046**M**
2.40	−9.477	3.048	−0.201	−1.472	0.092	5.981	0.809-0.085**M**	0.455-0.048**M**
2.45	−9.450	3.042	−0.201	−1.500	0.098	5.809	0.788-0.082**M**	0.447-0.047**M**
2.50	−9.378	3.022	−0.200	−1.529	0.105	5.560	0.780-0.081**M**	0.441-0.046**M**

DOI: 10.1002/eqe

Table I. *Continued*.

Period (s)	b_1	b_2	b_3	b_4	b_5	b_6	σ_1	σ_2
2.55	−9.263	2.986	−0.198	−1.560	0.112	5.249	0.772-0.079**M**	0.431-0.044**M**
2.60	−9.115	2.938	−0.195	−1.590	0.120	4.878	0.807-0.085**M**	0.456-0.048**M**
2.65	−8.937	2.878	−0.190	−1.613	0.127	4.416	0.846-0.091**M**	0.478-0.051**M**
2.70	−8.741	2.809	−0.185	−1.626	0.132	3.920	0.870-0.095**M**	0.492-0.053**M**
2.75	−8.559	2.742	−0.180	−1.625	0.135	3.460	0.885-0.097**M**	0.500-0.055**M**
2.80	−8.400	2.679	−0.174	−1.610	0.135	3.072	0.915-0.101**M**	0.513-0.057**M**
2.85	−8.267	2.623	−0.169	−1.574	0.131	2.797	0.945-0.105**M**	0.521-0.058**M**
2.90	−8.163	2.576	−0.164	−1.538	0.127	2.664	0.921-0.101**M**	0.503-0.055**M**
2.95	−8.083	2.539	−0.161	−1.502	0.122	2.650	0.892-0.097**M**	0.491-0.053**M**
3.00	−8.031	2.512	−0.158	−1.469	0.117	2.734	0.854-0.091**M**	0.471-0.050**M**
3.05	−7.909	2.466	−0.153	−1.437	0.111	2.862	0.829-0.086**M**	0.455-0.047**M**
3.10	−7.871	2.450	−0.151	−1.426	0.108	3.153	0.821-0.085**M**	0.444-0.046**M**
3.15	−8.004	2.488	−0.153	−1.430	0.108	3.316	0.831-0.086**M**	0.444-0.046**M**
3.20	−8.235	2.558	−0.158	−1.437	0.109	3.428	0.873-0.093**M**	0.462-0.049**M**
3.25	−8.489	2.635	−0.164	−1.448	0.110	3.497	0.736-0.071**M**	0.393-0.038**M**
3.30	−8.756	2.715	−0.170	−1.453	0.110	3.477	0.951-0.104**M**	0.490-0.054**M**
3.35	−9.060	2.806	−0.176	−1.456	0.111	3.434	0.994-0.110**M**	0.514-0.057**M**
3.40	−9.348	2.894	−0.183	−1.465	0.113	3.407	1.007-0.112**M**	0.514-0.057**M**
3.45	−9.654	2.984	−0.189	−1.464	0.113	3.357	1.123-0.129**M**	0.575-0.066**M**
3.50	−9.943	3.064	−0.195	−1.428	0.109	3.142	1.117-0.128**M**	0.572-0.066**M**
3.55	−10.204	3.133	−0.199	−1.392	0.105	3.005	1.155-0.134**M**	0.605-0.070**M**
3.60	−10.447	3.195	−0.203	−1.354	0.100	2.861	1.192-0.139**M**	0.628-0.073**M**
3.65	−10.694	3.259	−0.208	−1.313	0.096	2.716	1.488-0.181**M**	0.744-0.091**M**
3.70	−10.943	3.324	−0.212	−1.278	0.092	2.599	1.323-0.158**M**	0.668-0.080**M**
3.75	−11.164	3.378	−0.215	−1.236	0.087	2.478	1.371-0.165**M**	0.685-0.082**M**
3.80	−11.347	3.420	−0.218	−1.192	0.082	2.377	1.434-0.174**M**	0.710-0.086**M**
3.85	−11.493	3.453	−0.219	−1.154	0.077	2.329	1.484-0.181**M**	0.727-0.089**M**
3.90	−11.617	3.481	−0.221	−1.123	0.073	2.320	1.582-0.194**M**	0.772-0.095**M**
3.95	−11.735	3.507	−0.222	−1.093	0.069	2.311	1.598-0.196**M**	0.779-0.096**M**
4.00	−11.855	3.534	−0.224	−1.064	0.066	2.303	1.597-0.196**M**	0.775-0.095**M**

ordinates from normal and strike-slip events, which is consistent with previous observations (e.g. [26]). The motions from reverse-faulting events are stronger at short- and intermediate-periods, but become lower than those from the other mechanisms at longer periods; this is also consistent with previous observations that are discussed by Bommer *et al*. [26].

The two sets of equations produce broadly similar results up to 1.0 s for **M**6.0 and up to 2.0 s for **M**7.0, but confirm that that the ordinates at longer periods were significantly underestimated by the 1998 study, because of severe filters and, more importantly, the use of spectral ordinates at periods up to 0.1 s less than the filter cut-off. The new equations indicate that even for **M**6.0, the displacement plateau begins at a period of at least 3 s, whereas for **M**7.0 the corner period is significantly greater than 4 s.

4. IMPLICATIONS FOR EUROCODE 8

Implications of the new equations for the displacement spectra defined in EC8 are explored using the case of strike-slip earthquakes since our observations presented in Figure 6 have not revealed a

DOI: 10.1002/eqe

Table II. Regression coefficients b_1–b_6 for 5%-damped spectral ordinates (σ_1 and σ_2 denote the intra- and inter-event standard deviations, respectively).

Period (s)	b_1	b_2	b_3	b_4	b_5	b_6	σ_1	σ_2
0.05	−1.636	0.629	−0.070	−3.548	0.371	7.690	0.552-0.046**M**	0.210-0.018**M**
0.10	−0.692	0.582	−0.068	−3.462	0.360	8.248	0.652-0.062**M**	0.252-0.024**M**
0.15	−0.736	0.622	−0.064	−3.039	0.300	8.424	0.559-0.047**M**	0.226-0.019**M**
0.20	−1.556	0.833	−0.071	−2.637	0.241	8.291	0.445-0.027**M**	0.167-0.010**M**
0.25	−1.995	0.961	−0.078	−2.553	0.236	7.152	0.553-0.044**M**	0.173-0.014**M**
0.30	−2.616	1.156	−0.091	−2.468	0.225	6.819	0.625-0.055**M**	0.180-0.016**M**
0.35	−3.181	1.303	−0.099	−2.335	0.208	6.466	0.587-0.048**M**	0.176-0.014**M**
0.40	−3.425	1.386	−0.104	−2.350	0.209	6.562	0.603-0.050**M**	0.194-0.016**M**
0.45	−3.367	1.402	−0.107	−2.537	0.240	6.620	0.759-0.075**M**	0.237-0.023**M**
0.50	−3.936	1.552	−0.117	−2.442	0.228	6.052	0.868-0.091**M**	0.269-0.028**M**
0.55	−4.175	1.623	−0.122	−2.459	0.234	5.630	0.873-0.092**M**	0.294-0.031**M**
0.60	−4.339	1.672	−0.126	−2.495	0.243	5.181	0.929-0.102**M**	0.354-0.039**M**
0.65	−4.427	1.699	−0.128	−2.547	0.255	4.788	1.025-0.117**M**	0.396-0.045**M**
0.70	−4.466	1.707	−0.129	−2.584	0.263	4.497	1.157-0.137**M**	0.450-0.053**M**
0.75	−4.437	1.693	−0.127	−2.612	0.270	4.266	1.330-0.162**M**	0.470-0.057**M**
0.80	−4.385	1.674	−0.126	−2.646	0.277	4.156	1.707-0.215**M**	0.458-0.058**M**
0.85	−4.428	1.688	−0.126	−2.676	0.282	4.186	1.693-0.213**M**	0.449-0.057**M**
0.90	−4.589	1.734	−0.129	−2.668	0.280	4.292	1.594-0.200**M**	0.474-0.059**M**
0.95	−4.899	1.824	−0.135	−2.631	0.274	4.439	1.571-0.197**M**	0.467-0.058**M**
1.00	−5.256	1.925	−0.141	−2.575	0.264	4.582	1.380-0.170**M**	0.456-0.056**M**
1.05	−5.627	2.024	−0.147	−2.493	0.251	4.656	1.232-0.150**M**	0.449-0.055**M**
1.10	−5.993	2.117	−0.152	−2.390	0.234	4.694	1.088-0.128**M**	0.420-0.050**M**
1.15	−6.289	2.186	−0.154	−2.282	0.216	4.736	1.051-0.123**M**	0.425-0.050**M**
1.20	−6.516	2.233	−0.156	−2.178	0.199	4.789	1.007-0.116**M**	0.420-0.049**M**
1.25	−6.642	2.251	−0.155	−2.095	0.185	4.841	0.899-0.100**M**	0.391-0.044**M**
1.30	−6.682	2.245	−0.152	−2.029	0.174	4.878	0.882-0.098**M**	0.379-0.042**M**
1.35	−6.667	2.222	−0.149	−1.971	0.165	4.931	0.869-0.096**M**	0.383-0.042**M**
1.40	−6.667	2.206	−0.146	−1.917	0.156	5.000	0.901-0.101**M**	0.401-0.045**M**
1.45	−6.686	2.199	−0.144	−1.875	0.149	5.088	0.910-0.103**M**	0.414-0.047**M**
1.50	−6.724	2.205	−0.143	−1.857	0.146	5.189	0.936-0.107**M**	0.427-0.049**M**
1.55	−6.807	2.230	−0.145	−1.849	0.144	5.303	0.917-0.104**M**	0.413-0.047**M**
1.60	−6.944	2.273	−0.147	−1.843	0.142	5.435	0.912-0.103**M**	0.413-0.047**M**
1.65	−7.129	2.330	−0.151	−1.828	0.139	5.576	0.941-0.108**M**	0.443-0.051**M**
1.70	−7.331	2.393	−0.156	−1.810	0.136	5.737	0.933-0.106**M**	0.455-0.052**M**
1.75	−7.541	2.457	−0.160	−1.785	0.131	5.878	0.874-0.097**M**	0.443-0.049**M**
1.80	−7.744	2.518	−0.164	−1.753	0.125	6.003	0.826-0.089**M**	0.433-0.047**M**
1.85	−7.941	2.576	−0.167	−1.717	0.118	6.103	0.819-0.088**M**	0.435-0.047**M**
1.90	−8.116	2.626	−0.171	−1.679	0.112	6.185	0.785-0.083**M**	0.423-0.045**M**
1.95	−8.255	2.665	−0.173	−1.643	0.106	6.246	0.739-0.075**M**	0.403-0.041**M**
2.00	−8.352	2.693	−0.175	−1.617	0.101	6.274	0.723-0.073**M**	0.398-0.040**M**
2.05	−8.485	2.735	−0.178	−1.602	0.099	6.266	0.717-0.072**M**	0.397-0.040**M**
2.10	−8.610	2.776	−0.181	−1.598	0.100	6.222	0.700-0.069**M**	0.389-0.038**M**
2.15	−8.730	2.816	−0.184	−1.599	0.101	6.155	0.706-0.070**M**	0.392-0.039**M**
2.20	−8.811	2.843	−0.186	−1.600	0.103	6.044	0.751-0.078**M**	0.417-0.043**M**
2.25	−8.882	2.866	−0.188	−1.598	0.104	5.912	0.781-0.082**M**	0.436-0.046**M**
2.30	−8.942	2.884	−0.190	−1.591	0.105	5.761	0.788-0.084**M**	0.442-0.047**M**
2.35	−8.978	2.893	−0.191	−1.586	0.106	5.618	0.823-0.089**M**	0.460-0.050**M**
2.40	−8.969	2.890	−0.191	−1.586	0.107	5.478	0.832-0.090**M**	0.464-0.050**M**
2.45	−8.953	2.886	−0.191	−1.602	0.112	5.325	0.836-0.091**M**	0.470-0.051**M**
2.50	−8.903	2.871	−0.190	−1.622	0.116	5.160	0.817-0.088**M**	0.462-0.050**M**

DOI: 10.1002/eqe

Table II. *Continued*.

Period (s)	b_1	b_2	b_3	b_4	b_5	b_6	σ_1	σ_2
2.55	−8.822	2.846	−0.188	−1.643	0.121	4.954	0.835-0.091**M**	0.468-0.051**M**
2.60	−8.728	2.815	−0.186	−1.663	0.126	4.726	0.839-0.091**M**	0.478-0.052**M**
2.65	−8.613	2.776	−0.183	−1.680	0.131	4.467	0.855-0.093**M**	0.487-0.053**M**
2.70	−8.482	2.732	−0.180	−1.693	0.135	4.219	0.879-0.097**M**	0.499-0.055**M**
2.75	−8.355	2.686	−0.176	−1.696	0.137	3.984	0.890-0.098**M**	0.505-0.056**M**
2.80	−8.247	2.645	−0.172	−1.691	0.138	3.797	0.904-0.100**M**	0.511-0.057**M**
2.85	−8.134	2.598	−0.168	−1.666	0.135	3.639	0.902-0.100**M**	0.503-0.056**M**
2.90	−8.041	2.559	−0.164	−1.641	0.132	3.545	0.905-0.100**M**	0.501-0.055**M**
2.95	−7.966	2.526	−0.161	−1.614	0.129	3.516	0.875-0.095**M**	0.484-0.053**M**
3.00	−7.899	2.496	−0.158	−1.584	0.125	3.528	0.877-0.096**M**	0.481-0.052**M**
3.05	−7.831	2.466	−0.155	−1.555	0.120	3.551	0.846-0.091**M**	0.462-0.050**M**
3.10	−7.721	2.428	−0.151	−1.543	0.118	3.681	0.839-0.089**M**	0.458-0.049**M**
3.15	−7.911	2.484	−0.155	−1.546	0.119	3.715	0.850-0.091**M**	0.462-0.049**M**
3.20	−8.134	2.549	−0.160	−1.551	0.119	3.732	0.892-0.097**M**	0.481-0.052**M**
3.25	−8.381	2.624	−0.165	−1.559	0.120	3.739	0.765-0.078**M**	0.412-0.042**M**
3.30	−8.664	2.708	−0.171	−1.565	0.122	3.681	0.970-0.109**M**	0.518-0.058**M**
3.35	−8.937	2.789	−0.177	−1.570	0.123	3.598	0.985-0.111**M**	0.526-0.059**M**
3.40	−9.241	2.883	−0.184	−1.587	0.126	3.549	0.996-0.112**M**	0.527-0.059**M**
3.45	−9.482	2.956	−0.190	−1.595	0.128	3.485	1.107-0.129**M**	0.583-0.068**M**
3.50	−9.760	3.031	−0.195	−1.568	0.126	3.284	1.152-0.135**M**	0.601-0.071**M**
3.55	−9.932	3.075	−0.198	−1.542	0.123	3.162	1.128-0.131**M**	0.602-0.070**M**
3.60	−10.103	3.118	−0.201	−1.516	0.121	3.047	1.162-0.136**M**	0.623-0.073**M**
3.65	−10.267	3.158	−0.203	−1.486	0.117	2.932	1.448-0.177**M**	0.752-0.092**M**
3.70	−10.433	3.201	−0.206	−1.461	0.115	2.856	1.271-0.152**M**	0.666-0.080**M**
3.75	−10.578	3.234	−0.208	−1.429	0.111	2.784	1.286-0.154**M**	0.677-0.081**M**
3.80	−10.678	3.253	−0.208	−1.393	0.106	2.719	1.353-0.164**M**	0.706-0.085**M**
3.85	−10.770	3.270	−0.209	−1.357	0.102	2.681	1.345-0.162**M**	0.702-0.085**M**
3.90	−10.834	3.281	−0.209	−1.330	0.098	2.684	1.393-0.169**M**	0.737-0.089**M**
3.95	−10.899	3.292	−0.209	−1.304	0.095	2.688	1.411-0.171**M**	0.746-0.091**M**
4.00	−10.965	3.303	−0.209	−1.279	0.091	2.694	1.464-0.179**M**	0.768-0.094**M**

strong dependence of spectral displacement ordinates on the style-of-faulting. In order to be able to compare the predicted spectra with the displacement spectrum defined in EC8, it is necessary to estimate the PGA since the code uses this parameter. In order to be entirely consistent, we derived an equation for the geometric mean PGA using the same data and functional form, resulting in the following equation:

$$\log[\mathrm{PGA}] = 1.647 + 0.767\mathbf{M} - 0.074\mathbf{M}^2 + (-3.162 + 0.321\mathbf{M}) \log \sqrt{R_{\mathrm{jb}}^2 + 7.682^2} + 0.105 S_S + 0.020 S_A - 0.045 F_{\mathrm{N}} + 0.085 F_{\mathrm{R}} \quad (3)$$

The negative value of coefficient b_3 implies that for magnitudes above **M**7, the PGA not only saturates but actually starts to decrease with increasing magnitude. This is supported by the data and may be a general feature, perhaps related to predominantly greater slip in large earthquakes, although it could also simply reflect the specific characteristics of the few large events contributing

DOI: 10.1002/eqe

Table III. Regression coefficients b_1–b_6 for 10%-damped spectral ordinates (σ_1 and σ_2 denote the intra- and inter-event standard deviations, respectively).

Period (s)	b_1	b_2	b_3	b_4	b_5	b_6	σ_1	σ_2
0.05	−1.794	0.644	−0.070	−3.451	0.358	7.848	0.557-0.048**M**	0.201-0.017**M**
0.10	−1.003	0.630	−0.070	−3.384	0.350	8.185	0.599-0.054**M**	0.221-0.020**M**
0.15	−0.976	0.649	−0.065	−3.004	0.296	8.064	0.562-0.047**M**	0.218-0.018**M**
0.20	−1.628	0.840	−0.073	−2.719	0.254	7.955	0.492-0.035**M**	0.181-0.013**M**
0.25	−2.074	0.980	−0.081	−2.650	0.250	7.025	0.549-0.044**M**	0.172-0.014**M**
0.30	−2.522	1.109	−0.088	−2.541	0.235	6.744	0.633-0.057**M**	0.188-0.017**M**
0.35	−3.012	1.259	−0.098	−2.487	0.228	6.620	0.594-0.050**M**	0.184-0.015**M**
0.40	−3.340	1.355	−0.104	−2.453	0.223	6.403	0.617-0.053**M**	0.195-0.017**M**
0.45	−3.445	1.408	−0.109	−2.573	0.243	6.379	0.732-0.071**M**	0.227-0.022**M**
0.50	−3.767	1.496	−0.114	−2.537	0.240	6.040	0.815-0.084**M**	0.265-0.027**M**
0.55	−4.019	1.572	−0.119	−2.547	0.244	5.696	0.893-0.096**M**	0.308-0.033**M**
0.60	−4.200	1.626	−0.123	−2.576	0.251	5.320	0.927-0.102**M**	0.340-0.038**M**
0.65	−4.323	1.663	−0.126	−2.612	0.260	4.978	1.001-0.114**M**	0.384-0.044**M**
0.70	−4.411	1.688	−0.128	−2.643	0.267	4.697	1.064-0.124**M**	0.413-0.048**M**
0.75	−4.461	1.700	−0.129	−2.667	0.273	4.465	1.223-0.147**M**	0.446-0.054**M**
0.80	−4.508	1.710	−0.129	−2.685	0.278	4.323	1.358-0.167**M**	0.449-0.055**M**
0.85	−4.562	1.727	−0.130	−2.711	0.282	4.314	1.391-0.172**M**	0.447-0.055**M**
0.90	−4.706	1.770	−0.133	−2.714	0.283	4.389	1.408-0.174**M**	0.449-0.056**M**
0.95	−4.922	1.833	−0.137	−2.696	0.279	4.510	1.358-0.168**M**	0.449-0.055**M**
1.00	−5.185	1.908	−0.141	−2.655	0.272	4.656	1.364-0.169**M**	0.455-0.056**M**
1.05	−5.473	1.985	−0.146	−2.591	0.261	4.763	1.209-0.146**M**	0.437-0.053**M**
1.10	−5.748	2.053	−0.149	−2.509	0.247	4.836	1.128-0.135**M**	0.426-0.051**M**
1.15	−5.984	2.108	−0.151	−2.423	0.233	4.890	1.083-0.128**M**	0.424-0.050**M**
1.20	−6.159	2.144	−0.152	−2.346	0.220	4.930	1.014-0.118**M**	0.415-0.048**M**
1.25	−6.294	2.168	−0.152	−2.273	0.208	4.953	0.962-0.111**M**	0.407-0.047**M**
1.30	−6.368	2.175	−0.150	−2.213	0.199	4.973	0.933-0.106**M**	0.404-0.046**M**
1.35	−6.405	2.171	−0.148	−2.164	0.191	5.002	0.952-0.109**M**	0.422-0.048**M**
1.40	−6.438	2.169	−0.147	−2.120	0.184	5.037	0.945-0.109**M**	0.428-0.049**M**
1.45	−6.474	2.170	−0.146	−2.088	0.178	5.095	0.949-0.109**M**	0.435-0.050**M**
1.50	−6.530	2.183	−0.146	−2.070	0.175	5.181	0.966-0.112**M**	0.445-0.052**M**
1.55	−6.611	2.205	−0.147	−2.056	0.172	5.279	0.957-0.111**M**	0.441-0.051**M**
1.60	−6.728	2.238	−0.149	−2.040	0.169	5.366	0.959-0.111**M**	0.447-0.052**M**
1.65	−6.864	2.279	−0.151	−2.021	0.166	5.443	0.986-0.115**M**	0.471-0.055**M**
1.70	−7.016	2.324	−0.154	−2.002	0.163	5.520	0.975-0.113**M**	0.480-0.056**M**
1.75	−7.206	2.379	−0.158	−1.973	0.158	5.586	0.942-0.108**M**	0.478-0.055**M**
1.80	−7.403	2.436	−0.161	−1.939	0.152	5.636	0.918-0.104**M**	0.477-0.054**M**
1.85	−7.600	2.492	−0.165	−1.900	0.146	5.673	0.912-0.103**M**	0.476-0.054**M**
1.90	−7.779	2.542	−0.168	−1.858	0.139	5.695	0.808-0.087**M**	0.428-0.046**M**
1.95	−7.928	2.582	−0.170	−1.819	0.133	5.699	0.797-0.085**M**	0.422-0.045**M**
2.00	−8.040	2.612	−0.172	−1.787	0.128	5.695	0.774-0.082**M**	0.411-0.043**M**
2.05	−8.174	2.650	−0.174	−1.759	0.124	5.663	0.764-0.080**M**	0.410-0.043**M**
2.10	−8.298	2.685	−0.177	−1.734	0.121	5.613	0.779-0.083**M**	0.421-0.045**M**
2.15	−8.394	2.712	−0.178	−1.717	0.120	5.542	0.774-0.082**M**	0.423-0.045**M**
2.20	−8.440	2.724	−0.179	−1.704	0.119	5.452	0.834-0.092**M**	0.452-0.050**M**
2.25	−8.464	2.730	−0.180	−1.693	0.118	5.358	0.823-0.090**M**	0.447-0.049**M**
2.30	−8.472	2.730	−0.180	−1.684	0.118	5.262	0.850-0.094**M**	0.464-0.051**M**
2.35	−8.461	2.725	−0.179	−1.677	0.119	5.171	0.867-0.097**M**	0.471-0.053**M**
2.40	−8.428	2.713	−0.178	−1.673	0.119	5.077	0.879-0.099**M**	0.478-0.054**M**
2.45	−8.417	2.710	−0.178	−1.682	0.122	4.974	0.862-0.096**M**	0.473-0.053**M**
2.50	−8.394	2.703	−0.178	−1.695	0.125	4.863	0.860-0.096**M**	0.474-0.053**M**

DOI: 10.1002/eqe

Table III. *Continued.*

Period (s)	b_1	b_2	b_3	b_4	b_5	b_6	σ_1	σ_2
2.55	−8.361	2.694	−0.177	−1.710	0.128	4.753	0.882-0.099**M**	0.488-0.055**M**
2.60	−8.331	2.684	−0.176	−1.725	0.132	4.632	0.870-0.097**M**	0.488-0.054**M**
2.65	−8.289	2.670	−0.175	−1.738	0.135	4.504	0.879-0.098**M**	0.493-0.055**M**
2.70	−8.225	2.649	−0.174	−1.750	0.138	4.383	0.889-0.099**M**	0.496-0.056**M**
2.75	−8.149	2.622	−0.172	−1.754	0.140	4.266	0.924-0.105**M**	0.509-0.058**M**
2.80	−8.072	2.594	−0.169	−1.753	0.141	4.180	0.918-0.104**M**	0.506-0.057**M**
2.85	−7.971	2.555	−0.166	−1.737	0.139	4.096	0.932-0.106**M**	0.509-0.058**M**
2.90	−7.879	2.519	−0.162	−1.721	0.138	4.037	0.928-0.105**M**	0.509-0.057**M**
2.95	−7.799	2.487	−0.159	−1.702	0.135	3.993	0.897-0.100**M**	0.498-0.056**M**
3.00	−7.729	2.458	−0.156	−1.681	0.133	3.973	0.910-0.102**M**	0.503-0.056**M**
3.05	−7.661	2.430	−0.153	−1.660	0.130	3.954	0.891-0.099**M**	0.495-0.055**M**
3.10	−7.565	2.397	−0.151	−1.653	0.129	4.006	0.893-0.099**M**	0.496-0.055**M**
3.15	−7.737	2.448	−0.154	−1.660	0.130	3.975	0.886-0.098**M**	0.492-0.055**M**
3.20	−7.936	2.507	−0.158	−1.669	0.132	3.935	0.928-0.105**M**	0.514-0.058**M**
3.25	−8.158	2.575	−0.163	−1.681	0.134	3.902	0.807-0.086**M**	0.445-0.047**M**
3.30	−8.410	2.650	−0.169	−1.690	0.136	3.825	1.014-0.117**M**	0.561-0.065**M**
3.35	−8.655	2.722	−0.174	−1.695	0.137	3.732	1.019-0.117**M**	0.561-0.065**M**
3.40	−8.932	2.805	−0.180	−1.701	0.139	3.653	1.031-0.119**M**	0.561-0.065**M**
3.45	−9.149	2.867	−0.185	−1.697	0.139	3.567	1.146-0.136**M**	0.620-0.074**M**
3.50	−9.377	2.925	−0.189	−1.665	0.136	3.393	1.190-0.142**M**	0.635-0.076**M**
3.55	−9.504	2.954	−0.190	−1.636	0.133	3.289	1.209-0.145**M**	0.666-0.080**M**
3.60	−9.628	2.983	−0.192	−1.610	0.130	3.194	1.232-0.148**M**	0.682-0.082**M**
3.65	−9.746	3.009	−0.193	−1.583	0.127	3.102	1.420-0.175**M**	0.779-0.096**M**
3.70	−9.864	3.038	−0.195	−1.562	0.125	3.044	1.271-0.154**M**	0.703-0.085**M**
3.75	−9.973	3.062	−0.196	−1.536	0.122	2.987	1.267-0.153**M**	0.695-0.084**M**
3.80	−10.056	3.079	−0.197	−1.511	0.119	2.942	1.324-0.161**M**	0.720-0.087**M**
3.85	−10.149	3.099	−0.198	−1.489	0.117	2.917	1.329-0.161**M**	0.716-0.087**M**
3.90	−10.228	3.118	−0.199	−1.473	0.115	2.917	1.396-0.171**M**	0.755-0.092**M**
3.95	−10.308	3.136	−0.200	−1.457	0.113	2.919	1.383-0.169**M**	0.745-0.091**M**
4.00	−10.387	3.155	−0.201	−1.442	0.111	2.922	1.399-0.171**M**	0.751-0.092**M**

records to the data set. Since super-saturation of PGA with magnitude will be difficult for some users to accept, as it runs contrary to previous models, the regression was also repeated constraining b_3 to zero, yielding the following equation, which has a slightly larger variability:

$$\log[\mathrm{PGA}] = 4.185 - 0.112\mathbf{M} + (-2.963 + 0.290\mathbf{M}) \log\sqrt{R_{\mathrm{jb}}^2 + 7.593^2} + 0.099S_S + 0.020S_A - 0.034F_{\mathrm{N}} + 0.104F_{\mathrm{R}} \quad (4)$$

The magnitude-dependent intra- and inter-event standard deviations for Equation (3) are $\sigma_1 = 0.557–0.049\mathbf{M}$ and $\sigma_2 = 0.189–0.017\mathbf{M}$, respectively. The corresponding standard deviations for Equation (4) are $\sigma_1 = 0.557–0.049\mathbf{M}$ and $\sigma_2 = 0.204–0.018\mathbf{M}$. The predicted spectra are compared in Figures 7–9 with the 5%-damped Type 1 spectrum from EC8 anchored to the PGA value estimated using Equation (3). In each case, four different magnitudes from **M**6 to **M**7.5 and three site classes are considered; the three figures correspond to different source-to-site distances.

DOI: 10.1002/eqe

Table IV. Regression coefficients b_1–b_6 for 20%-damped spectral ordinates (σ_1 and σ_2 denote the intra- and inter-event standard deviations, respectively).

Period (s)	b_1	b_2	b_3	b_4	b_5	b_6	σ_1	σ_2
0.05	−1.947	0.658	−0.070	−3.364	0.348	7.931	0.568-0.050**M**	0.197-0.018**M**
0.10	−1.368	0.681	−0.071	−3.269	0.334	8.158	0.552-0.047**M**	0.192-0.016**M**
0.15	−1.433	0.734	−0.070	−2.953	0.290	7.859	0.545-0.045**M**	0.200-0.017**M**
0.20	−1.732	0.851	−0.076	−2.839	0.275	7.582	0.553-0.046**M**	0.189-0.016**M**
0.25	−2.215	1.008	−0.086	−2.765	0.268	6.935	0.574-0.049**M**	0.181-0.015**M**
0.30	−2.613	1.116	−0.090	−2.638	0.249	6.642	0.601-0.053**M**	0.186-0.016**M**
0.35	−2.879	1.199	−0.095	−2.591	0.242	6.563	0.607-0.053**M**	0.190-0.016**M**
0.40	−3.198	1.301	−0.101	−2.587	0.242	6.425	0.650-0.059**M**	0.205-0.019**M**
0.45	−3.406	1.378	−0.107	−2.641	0.250	6.421	0.714-0.069**M**	0.234-0.023**M**
0.50	−3.579	1.426	−0.110	−2.644	0.254	6.062	0.782-0.080**M**	0.265-0.027**M**
0.55	−3.795	1.494	−0.115	−2.657	0.258	5.808	0.901-0.099**M**	0.318-0.035**M**
0.60	−3.996	1.556	−0.119	−2.677	0.263	5.543	0.929-0.104**M**	0.346-0.039**M**
0.65	−4.169	1.608	−0.123	−2.694	0.268	5.288	0.956-0.108**M**	0.366-0.041**M**
0.70	−4.321	1.653	−0.126	−2.705	0.272	5.052	1.036-0.120**M**	0.392-0.046**M**
0.75	−4.456	1.690	−0.129	−2.712	0.275	4.857	1.098-0.130**M**	0.406-0.048**M**
0.80	−4.589	1.728	−0.131	−2.712	0.276	4.726	1.138-0.136**M**	0.415-0.050**M**
0.85	−4.721	1.765	−0.133	−2.712	0.277	4.666	1.161-0.140**M**	0.423-0.051**M**
0.90	−4.865	1.806	−0.136	−2.703	0.275	4.660	1.174-0.142**M**	0.431-0.052**M**
0.95	−5.025	1.849	−0.138	−2.682	0.272	4.697	1.180-0.143**M**	0.436-0.053**M**
1.00	−5.200	1.896	−0.140	−2.647	0.266	4.760	1.172-0.142**M**	0.437-0.053**M**
1.05	−5.379	1.942	−0.143	−2.605	0.259	4.829	1.122-0.135**M**	0.427-0.051**M**
1.10	−5.562	1.988	−0.145	−2.555	0.250	4.885	1.090-0.130**M**	0.421-0.050**M**
1.15	−5.733	2.029	−0.146	−2.501	0.241	4.922	1.041-0.123**M**	0.416-0.049**M**
1.20	−5.870	2.060	−0.147	−2.455	0.234	4.953	1.016-0.119**M**	0.419-0.049**M**
1.25	−5.978	2.083	−0.148	−2.413	0.227	4.977	0.963-0.111**M**	0.412-0.048**M**
1.30	−6.072	2.102	−0.148	−2.372	0.220	4.991	0.943-0.108**M**	0.413-0.047**M**
1.35	−6.145	2.115	−0.148	−2.338	0.215	5.009	0.981-0.114**M**	0.429-0.050**M**
1.40	−6.196	2.124	−0.148	−2.315	0.211	5.036	0.983-0.115**M**	0.438-0.051**M**
1.45	−6.234	2.131	−0.147	−2.298	0.208	5.078	0.945-0.109**M**	0.431-0.050**M**
1.50	−6.281	2.142	−0.147	−2.285	0.206	5.131	0.955-0.111**M**	0.440-0.051**M**
1.55	−6.343	2.158	−0.148	−2.270	0.203	5.189	0.975-0.114**M**	0.454-0.053**M**
1.60	−6.426	2.180	−0.149	−2.249	0.200	5.239	0.996-0.117**M**	0.469-0.055**M**
1.65	−6.524	2.206	−0.150	−2.226	0.196	5.285	0.995-0.117**M**	0.481-0.056**M**
1.70	−6.636	2.236	−0.152	−2.199	0.192	5.327	0.968-0.113**M**	0.477-0.056**M**
1.75	−6.776	2.273	−0.154	−2.167	0.187	5.345	0.956-0.111**M**	0.473-0.055**M**
1.80	−6.929	2.313	−0.156	−2.129	0.181	5.341	0.958-0.111**M**	0.479-0.056**M**
1.85	−7.087	2.354	−0.158	−2.089	0.176	5.316	0.933-0.107**M**	0.471-0.054**M**
1.90	−7.232	2.391	−0.161	−2.051	0.170	5.276	0.918-0.105**M**	0.473-0.054**M**
1.95	−7.359	2.423	−0.162	−2.015	0.165	5.227	0.900-0.102**M**	0.466-0.053**M**
2.00	−7.468	2.450	−0.164	−1.982	0.160	5.177	0.887-0.100**M**	0.463-0.052**M**
2.05	−7.600	2.485	−0.166	−1.951	0.156	5.116	0.886-0.100**M**	0.465-0.053**M**
2.10	−7.714	2.514	−0.168	−1.925	0.153	5.056	0.876-0.099**M**	0.462-0.052**M**
2.15	−7.799	2.535	−0.169	−1.902	0.150	4.999	0.856-0.096**M**	0.451-0.050**M**
2.20	−7.827	2.540	−0.169	−1.884	0.148	4.946	0.913-0.105**M**	0.474-0.054**M**
2.25	−7.829	2.537	−0.168	−1.868	0.147	4.898	0.909-0.104**M**	0.475-0.054**M**
2.30	−7.817	2.530	−0.167	−1.854	0.145	4.863	0.927-0.107**M**	0.486-0.056**M**
2.35	−7.792	2.519	−0.166	−1.842	0.144	4.832	0.933-0.108**M**	0.489-0.056**M**
2.40	−7.756	2.504	−0.165	−1.832	0.143	4.802	0.936-0.108**M**	0.493-0.057**M**
2.45	−7.747	2.501	−0.164	−1.832	0.144	4.750	0.915-0.105**M**	0.484-0.056**M**
2.50	−7.744	2.499	−0.164	−1.833	0.145	4.687	0.917-0.105**M**	0.490-0.056**M**

DOI: 10.1002/eqe

Table IV. *Continued*.

Period (s)	b_1	b_2	b_3	b_4	b_5	b_6	σ_1	σ_2
2.55	−7.744	2.498	−0.164	−1.834	0.146	4.614	0.923-0.106**M**	0.498-0.057**M**
2.60	−7.755	2.500	−0.164	−1.835	0.147	4.540	0.916-0.105**M**	0.502-0.057**M**
2.65	−7.755	2.498	−0.164	−1.835	0.148	4.463	0.925-0.106**M**	0.509-0.058**M**
2.70	−7.736	2.491	−0.163	−1.836	0.149	4.406	0.944-0.109**M**	0.520-0.060**M**
2.75	−7.708	2.481	−0.162	−1.836	0.149	4.363	0.951-0.110**M**	0.521-0.060**M**
2.80	−7.673	2.468	−0.161	−1.835	0.149	4.331	0.971-0.113**M**	0.532-0.062**M**
2.85	−7.612	2.445	−0.159	−1.824	0.148	4.299	0.960-0.111**M**	0.524-0.061**M**
2.90	−7.544	2.420	−0.156	−1.816	0.148	4.265	0.948-0.109**M**	0.520-0.060**M**
2.95	−7.477	2.395	−0.154	−1.807	0.147	4.231	0.957-0.111**M**	0.527-0.061**M**
3.00	−7.411	2.371	−0.152	−1.796	0.146	4.196	0.971-0.113**M**	0.537-0.062**M**
3.05	−7.348	2.347	−0.150	−1.784	0.144	4.158	0.982-0.114**M**	0.543-0.063**M**
3.10	−7.268	2.322	−0.147	−1.787	0.145	4.172	0.999-0.117**M**	0.553-0.065**M**
3.15	−7.415	2.365	−0.151	−1.796	0.147	4.125	1.018-0.120**M**	0.563-0.066**M**
3.20	−7.590	2.418	−0.154	−1.805	0.149	4.080	1.076-0.128**M**	0.590-0.070**M**
3.25	−7.787	2.477	−0.159	−1.816	0.151	4.043	0.890-0.100**M**	0.486-0.055**M**
3.30	−8.012	2.543	−0.164	−1.819	0.152	3.972	1.142-0.137**M**	0.632-0.076**M**
3.35	−8.234	2.607	−0.168	−1.820	0.153	3.892	1.130-0.135**M**	0.622-0.075**M**
3.40	−8.491	2.684	−0.174	−1.827	0.154	3.842	1.139-0.137**M**	0.622-0.075**M**
3.45	−8.694	2.744	−0.179	−1.828	0.155	3.788	1.311-0.161**M**	0.703-0.086**M**
3.50	−8.904	2.797	−0.182	−1.801	0.153	3.644	1.352-0.167**M**	0.712-0.088**M**
3.55	−9.015	2.824	−0.184	−1.785	0.151	3.566	1.276-0.156**M**	0.703-0.086**M**
3.60	−9.127	2.852	−0.186	−1.769	0.150	3.485	1.300-0.159**M**	0.713-0.087**M**
3.65	−9.235	2.878	−0.187	−1.752	0.148	3.399	1.569-0.197**M**	0.830-0.104**M**
3.70	−9.345	2.906	−0.189	−1.739	0.147	3.337	1.308-0.160**M**	0.724-0.088**M**
3.75	−9.448	2.931	−0.190	−1.720	0.146	3.272	1.352-0.166**M**	0.738-0.091**M**
3.80	−9.527	2.948	−0.191	−1.700	0.143	3.204	1.410-0.174**M**	0.760-0.094**M**
3.85	−9.614	2.968	−0.192	−1.685	0.142	3.152	1.410-0.174**M**	0.753-0.093**M**
3.90	−9.693	2.988	−0.194	−1.674	0.141	3.124	1.461-0.181**M**	0.777-0.096**M**
3.95	−9.772	3.008	−0.195	−1.663	0.140	3.097	1.465-0.182**M**	0.775-0.096**M**
4.00	−9.852	3.029	−0.196	−1.653	0.139	3.070	1.469-0.182**M**	0.773-0.096**M**

A number of interesting observations can be made and are equally applicable to all three figures. The main and most important observation is that a spectrum defined on the basis of a single ground-motion parameter simply cannot model the variation of spectral shape with magnitude. Using PGA as the anchor parameter leads to serious under- and over-estimation of the intermediate- and long-period spectral ordinates; considering the ordinates up to 2 s, the EC8 spectrum seems to be well adjusted for a magnitude **M**7 earthquake, but is conservative for smaller events and underestimates the ordinates for a magnitude **M**7.5 earthquake. The mismatch is particularly marked at longer periods because of the entirely inappropriate choice of 2 s as the corner period for the EC8 spectrum. The results seem to indicate a corner period of about 3.5 s even at **M**6.5, and values considerably greater than 4 s for larger events, which is consistent with recent models for displacement spectra such as that proposed in NEHRP 2003. In fact, for **M**6.5, the equation provided in NEHRP 2003 suggests a corner period at 5.6 s.

Since the new predictive equations have been derived for spectral displacements at various damping levels, they can also be used to assess the scaling factors used to obtain spectral ordinates

DOI: 10.1002/eqe

Table V. Regression coefficients b_1–b_6 for 30%-damped spectral ordinates (σ_1 and σ_2 denote the intra- and inter-event standard deviations, respectively).

Period (s)	b_1	b_2	b_3	b_4	b_5	b_6	σ_1	σ_2
0.05	−2.077	0.674	−0.070	−3.298	0.339	7.955	0.563-0.050**M**	0.191-0.017**M**
0.10	−1.547	0.694	−0.071	−3.203	0.326	8.057	0.561-0.049**M**	0.189-0.017**M**
0.15	−1.646	0.769	−0.072	−2.965	0.293	7.781	0.547-0.046**M**	0.192-0.016**M**
0.20	−1.971	0.903	−0.080	−2.885	0.282	7.471	0.559-0.047**M**	0.188-0.016**M**
0.25	−2.382	1.034	−0.087	−2.788	0.270	6.959	0.580-0.050**M**	0.185-0.016**M**
0.30	−2.643	1.108	−0.090	−2.701	0.258	6.682	0.605-0.054**M**	0.189-0.017**M**
0.35	−2.896	1.188	−0.095	−2.663	0.252	6.558	0.620-0.055**M**	0.198-0.018**M**
0.40	−3.211	1.296	−0.102	−2.670	0.253	6.498	0.658-0.061**M**	0.219-0.020**M**
0.45	−3.405	1.367	−0.107	−2.712	0.261	6.402	0.725-0.072**M**	0.248-0.025**M**
0.50	−3.489	1.390	−0.109	−2.728	0.266	6.080	0.798-0.083**M**	0.275-0.029**M**
0.55	−3.696	1.455	−0.113	−2.735	0.269	5.873	0.855-0.093**M**	0.311-0.034**M**
0.60	−3.887	1.515	−0.117	−2.747	0.273	5.662	0.953-0.108**M**	0.350-0.040**M**
0.65	−4.074	1.571	−0.121	−2.752	0.275	5.455	1.001-0.116**M**	0.370-0.043**M**
0.70	−4.243	1.621	−0.124	−2.753	0.277	5.267	0.966-0.111**M**	0.370-0.042**M**
0.75	−4.403	1.666	−0.127	−2.750	0.278	5.111	1.038-0.122**M**	0.389-0.046**M**
0.80	−4.559	1.710	−0.130	−2.742	0.278	4.990	1.048-0.123**M**	0.396-0.047**M**
0.85	−4.712	1.753	−0.133	−2.729	0.276	4.914	1.091-0.130**M**	0.409-0.049**M**
0.90	−4.855	1.792	−0.135	−2.713	0.274	4.876	1.098-0.131**M**	0.418-0.050**M**
0.95	−4.982	1.826	−0.137	−2.693	0.271	4.873	1.092-0.130**M**	0.422-0.050**M**
1.00	−5.115	1.860	−0.138	−2.663	0.266	4.896	1.087-0.130**M**	0.422-0.050**M**
1.05	−5.240	1.892	−0.139	−2.633	0.261	4.934	1.066-0.127**M**	0.423-0.050**M**
1.10	−5.360	1.922	−0.140	−2.601	0.255	4.974	1.041-0.123**M**	0.421-0.050**M**
1.15	−5.479	1.951	−0.142	−2.567	0.249	5.003	1.010-0.119**M**	0.419-0.049**M**
1.20	−5.582	1.975	−0.142	−2.534	0.244	5.028	1.002-0.117**M**	0.426-0.050**M**
1.25	−5.672	1.995	−0.143	−2.504	0.239	5.048	0.992-0.116**M**	0.432-0.051**M**
1.30	−5.748	2.012	−0.143	−2.476	0.235	5.064	0.963-0.112**M**	0.429-0.050**M**
1.35	−5.825	2.028	−0.143	−2.447	0.230	5.070	0.968-0.113**M**	0.436-0.051**M**
1.40	−5.900	2.045	−0.144	−2.419	0.226	5.071	0.972-0.113**M**	0.443-0.052**M**
1.45	−5.980	2.062	−0.144	−2.390	0.222	5.069	0.983-0.115**M**	0.453-0.053**M**
1.50	−6.049	2.078	−0.145	−2.371	0.219	5.082	0.956-0.111**M**	0.450-0.052**M**
1.55	−6.118	2.096	−0.145	−2.353	0.216	5.101	0.945-0.109**M**	0.449-0.052**M**
1.60	−6.193	2.114	−0.146	−2.335	0.213	5.124	0.931-0.107**M**	0.447-0.052**M**
1.65	−6.275	2.135	−0.147	−2.314	0.210	5.145	1.013-0.120**M**	0.489-0.058**M**
1.70	−6.364	2.158	−0.148	−2.290	0.207	5.158	1.002-0.118**M**	0.489-0.058**M**
1.75	−6.464	2.183	−0.149	−2.265	0.203	5.153	1.001-0.118**M**	0.491-0.058**M**
1.80	−6.571	2.210	−0.151	−2.237	0.199	5.136	0.982-0.115**M**	0.486-0.057**M**
1.85	−6.669	2.234	−0.152	−2.208	0.195	5.110	0.968-0.113**M**	0.484-0.057**M**
1.90	−6.774	2.258	−0.153	−2.175	0.191	5.072	0.972-0.114**M**	0.491-0.057**M**
1.95	−6.870	2.281	−0.154	−2.144	0.186	5.030	0.954-0.111**M**	0.486-0.057**M**
2.00	−6.953	2.299	−0.155	−2.114	0.182	4.981	0.972-0.114**M**	0.498-0.058**M**
2.05	−7.063	2.327	−0.156	−2.085	0.178	4.929	0.954-0.111**M**	0.491-0.057**M**
2.10	−7.162	2.351	−0.158	−2.058	0.175	4.877	0.950-0.111**M**	0.489-0.057**M**
2.15	−7.250	2.372	−0.159	−2.033	0.172	4.832	0.956-0.112**M**	0.494-0.058**M**
2.20	−7.284	2.378	−0.159	−2.013	0.169	4.786	1.009-0.120**M**	0.514-0.061**M**
2.25	−7.302	2.379	−0.159	−1.994	0.167	4.744	1.008-0.119**M**	0.516-0.061**M**
2.30	−7.305	2.376	−0.158	−1.978	0.166	4.706	0.981-0.115**M**	0.505-0.059**M**
2.35	−7.295	2.370	−0.157	−1.964	0.164	4.673	0.993-0.117**M**	0.513-0.061**M**
2.40	−7.277	2.360	−0.156	−1.951	0.163	4.647	1.000-0.118**M**	0.520-0.062**M**
2.45	−7.277	2.359	−0.156	−1.947	0.163	4.608	0.982-0.116**M**	0.512-0.060**M**
2.50	−7.281	2.359	−0.155	−1.944	0.163	4.564	0.982-0.116**M**	0.515-0.061**M**

DOI: 10.1002/eqe

Table V. *Continued*.

Period (s)	b_1	b_2	b_3	b_4	b_5	b_6	σ_1	σ_2
2.55	−7.291	2.360	−0.155	−1.941	0.163	4.519	0.982-0.116**M**	0.517-0.061**M**
2.60	−7.317	2.367	−0.156	−1.936	0.162	4.476	0.990-0.117**M**	0.529-0.062**M**
2.65	−7.337	2.371	−0.156	−1.930	0.162	4.432	1.011-0.120**M**	0.543-0.064**M**
2.70	−7.344	2.372	−0.156	−1.927	0.162	4.408	0.998-0.118**M**	0.538-0.063**M**
2.75	−7.340	2.369	−0.155	−1.924	0.162	4.391	1.004-0.119**M**	0.541-0.064**M**
2.80	−7.330	2.366	−0.155	−1.921	0.162	4.380	1.022-0.121**M**	0.551-0.065**M**
2.85	−7.298	2.353	−0.153	−1.912	0.161	4.368	0.993-0.117**M**	0.537-0.063**M**
2.90	−7.258	2.339	−0.152	−1.908	0.160	4.356	1.003-0.118**M**	0.543-0.064**M**
2.95	−7.217	2.325	−0.151	−1.906	0.160	4.348	1.008-0.119**M**	0.548-0.065**M**
3.00	−7.176	2.311	−0.150	−1.904	0.160	4.335	1.032-0.123**M**	0.561-0.066**M**
3.05	−7.136	2.297	−0.148	−1.900	0.160	4.315	1.040-0.124**M**	0.565-0.067**M**
3.10	−7.079	2.281	−0.147	−1.909	0.162	4.329	1.023-0.121**M**	0.558-0.066**M**
3.15	−7.223	2.327	−0.151	−1.927	0.165	4.306	1.069-0.128**M**	0.579-0.069**M**
3.20	−7.387	2.377	−0.154	−1.942	0.167	4.274	1.149-0.140**M**	0.611-0.074**M**
3.25	−7.569	2.434	−0.159	−1.959	0.170	4.251	0.944-0.109**M**	0.502-0.058**M**
3.30	−7.780	2.498	−0.164	−1.970	0.172	4.201	1.154-0.140**M**	0.622-0.075**M**
3.35	−7.991	2.560	−0.168	−1.975	0.174	4.134	1.201-0.146**M**	0.644-0.079**M**
3.40	−8.233	2.633	−0.174	−1.986	0.176	4.100	1.191-0.145**M**	0.634-0.077**M**
3.45	−8.426	2.690	−0.178	−1.990	0.177	4.067	1.349-0.167**M**	0.701-0.087**M**
3.50	−8.618	2.739	−0.181	−1.966	0.175	3.955	1.434-0.179**M**	0.724-0.090**M**
3.55	−8.725	2.763	−0.183	−1.945	0.173	3.874	1.329-0.164**M**	0.713-0.088**M**
3.60	−8.826	2.786	−0.184	−1.926	0.171	3.798	1.337-0.165**M**	0.720-0.089**M**
3.65	−8.915	2.807	−0.185	−1.908	0.169	3.723	1.567-0.197**M**	0.818-0.103**M**
3.70	−9.002	2.828	−0.186	−1.899	0.168	3.674	1.457-0.182**M**	0.782-0.098**M**
3.75	−9.082	2.848	−0.187	−1.887	0.168	3.621	1.437-0.179**M**	0.774-0.096**M**
3.80	−9.141	2.860	−0.188	−1.875	0.167	3.559	1.428-0.178**M**	0.770-0.096**M**
3.85	−9.218	2.879	−0.189	−1.863	0.166	3.491	1.396-0.173**M**	0.752-0.093**M**
3.90	−9.287	2.897	−0.190	−1.860	0.166	3.456	1.435-0.179**M**	0.777-0.097**M**
3.95	−9.355	2.916	−0.192	−1.857	0.166	3.420	1.438-0.179**M**	0.775-0.096**M**
4.00	−9.424	2.935	−0.193	−1.855	0.166	3.386	1.524-0.191**M**	0.799-0.100**M**

for damping ratios other than 5% of critical. The factors are applied between control periods T_B and T_E, and then converge to 1 at $T = 0$ and $T = T_F$ (Figure 1). In the 1994 edition of EC8, the scaling factor was given by the following equation:

$$\frac{\mathrm{SD}(\xi\%)}{\mathrm{SD}(5\%)} = \sqrt{\frac{7}{2+\xi}} \tag{5}$$

In the 2004 version of the code, this was replaced by the expression presented in Equation (1) derived by Bommer *et al*. [15]. Recently, Bommer and Mendis [17] compared scaling factors from various codes and publications, and found a surprising degree of divergence. This led to an investigation of the factors influencing the scaling factors, and it was found that the amount of reduction of the 5%-damped ordinates for higher damping values increased with both magnitude and distance, indicating a dependence on duration.

In Figures 10 and 11, the ratios of spectral ordinates at different damping levels obtained from the new equations are shown for various combinations of magnitude and distance; in all the cases,

DOI: 10.1002/eqe

Table VI. Regression coefficients b_7–b_{10} for all damping values.

Period	b_7	b_8	b_9	b_{10}	Period	b_7	b_8	b_9	b_{10}
2%- and 5%-damped spectra									
0.05	0.062	−0.018	−0.047	0.084	2.05	0.322	0.143	−0.011	0.007
0.10	0.036	0.006	−0.049	0.084	2.10	0.318	0.140	−0.014	0.003
0.15	0.039	0.021	−0.048	0.086	2.15	0.314	0.137	−0.017	0.001
0.20	0.068	0.031	−0.047	0.087	2.20	0.312	0.134	−0.020	−0.002
0.25	0.111	0.039	−0.047	0.088	2.25	0.310	0.131	−0.022	−0.003
0.30	0.146	0.049	−0.045	0.090	2.30	0.308	0.128	−0.023	−0.005
0.35	0.184	0.064	−0.041	0.093	2.35	0.306	0.126	−0.024	−0.006
0.40	0.227	0.086	−0.037	0.096	2.40	0.304	0.124	−0.024	−0.007
0.45	0.266	0.106	−0.033	0.097	2.45	0.301	0.122	−0.025	−0.008
0.50	0.266	0.105	−0.027	0.099	2.50	0.298	0.119	−0.026	−0.009
0.55	0.288	0.113	−0.021	0.101	2.55	0.295	0.116	−0.027	−0.010
0.60	0.310	0.120	−0.015	0.103	2.60	0.291	0.113	−0.027	−0.011
0.65	0.329	0.124	−0.007	0.103	2.65	0.288	0.109	−0.027	−0.012
0.70	0.345	0.129	0.001	0.102	2.70	0.284	0.106	−0.027	−0.012
0.75	0.359	0.133	0.009	0.102	2.75	0.281	0.102	−0.027	−0.013
0.80	0.370	0.137	0.016	0.101	2.80	0.278	0.099	−0.026	−0.014
0.85	0.379	0.140	0.022	0.099	2.85	0.275	0.096	−0.026	−0.014
0.90	0.387	0.144	0.025	0.097	2.90	0.273	0.094	−0.025	−0.016
0.95	0.393	0.148	0.026	0.092	2.95	0.270	0.092	−0.025	−0.019
1.00	0.398	0.152	0.025	0.087	3.00	0.268	0.089	−0.025	−0.021
1.05	0.401	0.156	0.024	0.080	3.05	0.265	0.086	−0.024	−0.024
1.10	0.403	0.159	0.021	0.073	3.10	0.262	0.084	−0.024	−0.027
1.15	0.403	0.163	0.018	0.067	3.15	0.262	0.081	−0.018	−0.036
1.20	0.403	0.166	0.015	0.061	3.20	0.262	0.078	−0.011	−0.045
1.25	0.400	0.168	0.012	0.057	3.25	0.262	0.075	−0.004	−0.055
1.30	0.397	0.169	0.011	0.053	3.30	0.262	0.072	0.003	−0.063
1.35	0.391	0.170	0.010	0.050	3.35	0.263	0.069	0.009	−0.070
1.40	0.385	0.169	0.010	0.047	3.40	0.264	0.067	0.015	−0.077
1.45	0.379	0.167	0.010	0.044	3.45	0.266	0.065	0.020	−0.083
1.50	0.373	0.164	0.011	0.041	3.50	0.267	0.063	0.024	−0.086
1.55	0.367	0.161	0.011	0.039	3.55	0.267	0.061	0.025	−0.088
1.60	0.361	0.158	0.010	0.036	3.60	0.266	0.060	0.026	−0.089
1.65	0.356	0.156	0.009	0.034	3.65	0.264	0.058	0.027	−0.090
1.70	0.351	0.154	0.008	0.031	3.70	0.262	0.057	0.029	−0.092
1.75	0.347	0.153	0.007	0.028	3.75	0.260	0.056	0.031	−0.093
1.80	0.343	0.151	0.004	0.024	3.80	0.257	0.055	0.032	−0.092
1.85	0.338	0.150	0.002	0.021	3.85	0.254	0.055	0.034	−0.089
1.90	0.334	0.149	−0.001	0.017	3.90	0.251	0.055	0.036	−0.088
1.95	0.330	0.148	−0.005	0.014	3.95	0.248	0.054	0.038	−0.086
2.00	0.327	0.146	−0.008	0.010	4.00	0.244	0.054	0.039	−0.084
10%-damped spectrum									
0.05	0.062	−0.018	−0.047	0.084	2.05	0.322	0.143	−0.011	0.007
0.10	0.036	0.006	−0.049	0.084	2.10	0.318	0.140	−0.014	0.003
0.15	0.039	0.021	−0.048	0.086	2.15	0.314	0.137	−0.017	0.001
0.20	0.068	0.031	−0.047	0.087	2.20	0.312	0.134	−0.020	−0.002
0.25	0.111	0.039	−0.047	0.088	2.25	0.310	0.131	−0.022	−0.003
0.30	0.146	0.049	−0.045	0.090	2.30	0.308	0.128	−0.023	−0.005
0.35	0.184	0.064	−0.041	0.093	2.35	0.306	0.126	−0.024	−0.006
0.40	0.227	0.086	−0.037	0.096	2.40	0.304	0.124	−0.024	−0.007
0.45	0.266	0.106	−0.033	0.097	2.45	0.301	0.122	−0.025	−0.008

DOI: 10.1002/eqe

Table VI. *Continued*.

Period	b_7	b_8	b_9	b_{10}	Period	b_7	b_8	b_9	b_{10}
0.50	0.266	0.105	−0.027	0.099	2.50	0.298	0.119	−0.026	−0.009
0.55	0.288	0.113	−0.021	0.101	2.55	0.295	0.116	−0.027	−0.010
0.60	0.310	0.120	−0.015	0.103	2.60	0.291	0.113	−0.027	−0.011
0.65	0.329	0.124	−0.007	0.103	2.65	0.288	0.109	−0.027	−0.012
0.70	0.345	0.129	0.001	0.102	2.70	0.284	0.106	−0.027	−0.012
0.75	0.359	0.133	0.009	0.102	2.75	0.281	0.102	−0.027	−0.013
0.80	0.370	0.137	0.016	0.101	2.80	0.278	0.099	−0.026	−0.014
0.85	0.379	0.140	0.022	0.099	2.85	0.275	0.096	−0.026	−0.014
0.90	0.387	0.144	0.025	0.097	2.90	0.273	0.094	−0.025	−0.015
0.95	0.393	0.148	0.026	0.092	2.95	0.270	0.092	−0.025	−0.016
1.00	0.398	0.152	0.025	0.087	3.00	0.268	0.089	−0.025	−0.017
1.05	0.401	0.156	0.024	0.080	3.05	0.265	0.086	−0.024	−0.018
1.10	0.403	0.159	0.021	0.073	3.10	0.262	0.084	−0.024	−0.020
1.15	0.403	0.163	0.018	0.067	3.15	0.262	0.081	−0.018	−0.027
1.20	0.403	0.166	0.015	0.061	3.20	0.262	0.078	−0.011	−0.034
1.25	0.400	0.168	0.012	0.057	3.25	0.262	0.075	−0.004	−0.041
1.30	0.397	0.169	0.011	0.053	3.30	0.262	0.072	0.003	−0.047
1.35	0.391	0.170	0.010	0.050	3.35	0.263	0.069	0.009	−0.051
1.40	0.385	0.169	0.010	0.047	3.40	0.264	0.067	0.015	−0.056
1.45	0.379	0.167	0.010	0.044	3.45	0.266	0.065	0.020	−0.060
1.50	0.373	0.164	0.011	0.041	3.50	0.267	0.063	0.024	−0.061
1.55	0.367	0.161	0.011	0.039	3.55	0.267	0.061	0.025	−0.061
1.60	0.361	0.158	0.010	0.036	3.60	0.266	0.060	0.026	−0.062
1.65	0.356	0.156	0.009	0.034	3.65	0.264	0.058	0.027	−0.062
1.70	0.351	0.154	0.008	0.031	3.70	0.262	0.057	0.029	−0.063
1.75	0.347	0.153	0.007	0.028	3.75	0.260	0.056	0.031	−0.063
1.80	0.343	0.151	0.004	0.024	3.80	0.257	0.055	0.032	−0.062
1.85	0.338	0.150	0.002	0.021	3.85	0.254	0.055	0.034	−0.061
1.90	0.334	0.149	−0.001	0.017	3.90	0.251	0.055	0.036	−0.061
1.95	0.330	0.148	−0.005	0.014	3.95	0.248	0.054	0.038	−0.060
2.00	0.327	0.146	−0.008	0.010	4.00	0.244	0.054	0.039	−0.060
20%- and 30%-damped spectra									
0.05	0.090	0.007	−0.047	0.084	2.05	0.322	0.143	−0.011	0.007
0.10	0.076	0.015	−0.049	0.084	2.10	0.318	0.140	−0.014	0.003
0.15	0.083	0.023	−0.048	0.086	2.15	0.314	0.137	−0.017	0.001
0.20	0.107	0.033	−0.047	0.087	2.20	0.312	0.134	−0.020	−0.002
0.25	0.138	0.044	−0.047	0.088	2.25	0.310	0.131	−0.022	−0.003
0.30	0.165	0.054	−0.045	0.090	2.30	0.308	0.128	−0.023	−0.005
0.35	0.193	0.068	−0.041	0.093	2.35	0.306	0.126	−0.024	−0.006
0.40	0.220	0.084	−0.037	0.096	2.40	0.304	0.124	−0.024	−0.007
0.45	0.243	0.097	−0.033	0.097	2.45	0.301	0.122	−0.025	−0.008
0.50	0.266	0.105	−0.027	0.099	2.50	0.298	0.119	−0.026	−0.009
0.55	0.288	0.113	−0.021	0.101	2.55	0.295	0.116	−0.027	−0.010
0.60	0.310	0.120	−0.015	0.103	2.60	0.291	0.113	−0.027	−0.011
0.65	0.329	0.124	−0.007	0.103	2.65	0.288	0.109	−0.027	−0.012
0.70	0.345	0.129	0.001	0.102	2.70	0.284	0.106	−0.027	−0.012
0.75	0.359	0.133	0.009	0.102	2.75	0.281	0.102	−0.027	−0.013
0.80	0.370	0.137	0.016	0.101	2.80	0.278	0.099	−0.026	−0.014
0.85	0.379	0.140	0.022	0.099	2.85	0.275	0.096	−0.026	−0.014
0.90	0.387	0.144	0.025	0.097	2.90	0.273	0.094	−0.025	−0.014
0.95	0.393	0.148	0.026	0.092	2.95	0.270	0.092	−0.025	−0.014

DOI: 10.1002/eqe

Table VI. *Continued*.

Period	b_7	b_8	b_9	b_{10}	Period	b_7	b_8	b_9	b_{10}
1.00	0.398	0.152	0.025	0.087	3.00	0.268	0.089	−0.025	−0.013
1.05	0.401	0.156	0.024	0.080	3.05	0.265	0.086	−0.024	−0.012
1.10	0.403	0.159	0.021	0.073	3.10	0.262	0.084	−0.024	−0.013
1.15	0.403	0.163	0.018	0.067	3.15	0.262	0.081	−0.018	−0.017
1.20	0.403	0.166	0.015	0.061	3.20	0.262	0.078	−0.011	−0.020
1.25	0.400	0.168	0.012	0.057	3.25	0.262	0.075	−0.004	−0.024
1.30	0.397	0.169	0.011	0.053	3.30	0.262	0.072	0.003	−0.026
1.35	0.391	0.170	0.010	0.050	3.35	0.263	0.069	0.009	−0.027
1.40	0.385	0.169	0.010	0.047	3.40	0.264	0.067	0.015	−0.029
1.45	0.379	0.167	0.010	0.044	3.45	0.266	0.065	0.020	−0.030
1.50	0.373	0.164	0.011	0.041	3.50	0.267	0.063	0.024	−0.027
1.55	0.367	0.161	0.011	0.039	3.55	0.267	0.061	0.025	−0.025
1.60	0.361	0.158	0.010	0.036	3.60	0.266	0.060	0.026	−0.024
1.65	0.356	0.156	0.009	0.034	3.65	0.264	0.058	0.027	−0.022
1.70	0.351	0.154	0.008	0.031	3.70	0.262	0.057	0.029	−0.023
1.75	0.347	0.153	0.007	0.028	3.75	0.260	0.056	0.031	−0.023
1.80	0.343	0.151	0.004	0.024	3.80	0.257	0.055	0.032	−0.023
1.85	0.338	0.150	0.002	0.021	3.85	0.254	0.055	0.034	−0.023
1.90	0.334	0.149	−0.001	0.017	3.90	0.251	0.055	0.036	−0.025
1.95	0.330	0.148	−0.005	0.014	3.95	0.248	0.054	0.038	−0.027
2.00	0.327	0.146	−0.008	0.010	4.00	0.244	0.054	0.039	−0.028

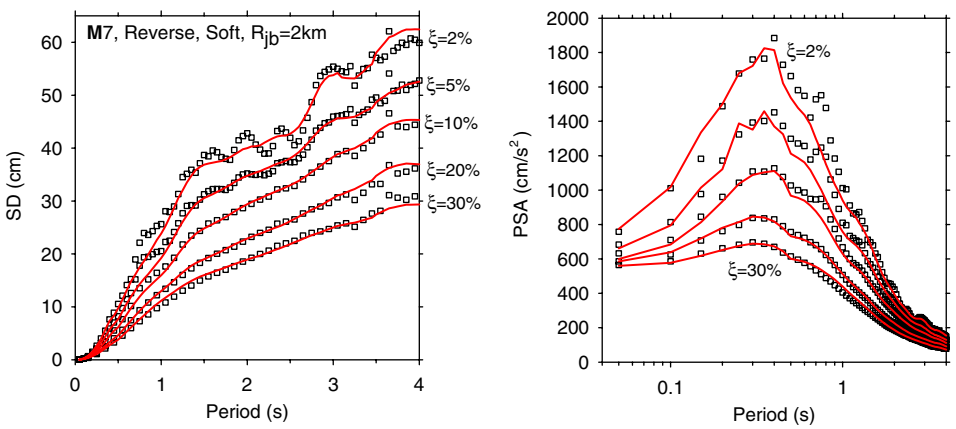

Figure 5. Spectral displacement (left) and corresponding pseudo-spectral acceleration (right) predictions at different damping levels using soft-site raw and smoothed regression coefficients for a reverse faulting scenario event of **M**7 and $R_{\text{jb}} = 2\,\text{km}$.

the ratios are for strike-slip faulting and stiff soil sites, although the coefficients for site class and style-of-faulting were found to have little influence on the damping dependence. The values obtained from the equations are compared to those from Equations (1) and (5).

DOI: 10.1002/eqe

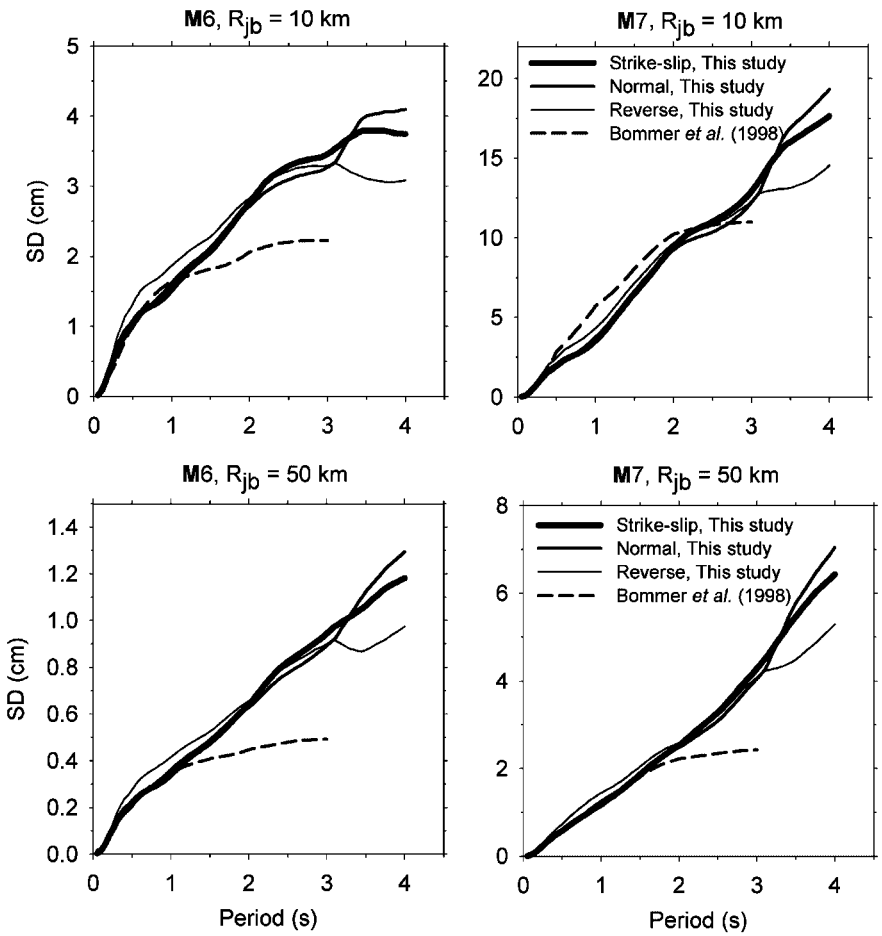

Figure 6. Comparison between the new predictive equations and Bommer *et al*. [23].

Figures 10 and 11 suggest that for the magnitude–distance combinations shown, which are likely to cover those of greatest engineering significance, the current EC8 scaling factors are a clear improvement on those from the earlier edition, at least at the longer periods of relevance to displacement-based design. The results also confirm the magnitude and distance dependence identified by Bommer and Mendis [17]; for periods beyond 3 s, the dependence of the scaling factors on duration appears to be very marked.

The comparisons made in this paper lead to a series of conclusions regarding urgently needed modifications to the displacement response spectra defined in EC8, confirming the statements made by Bommer and Pinho [5]:

- The spectrum cannot be constructed on the basis of a single parameter (PGA), and at least three (and possibly even more) parameters will be required to construct the uniform hazard displacement spectrum.

DOI: 10.1002/eqe

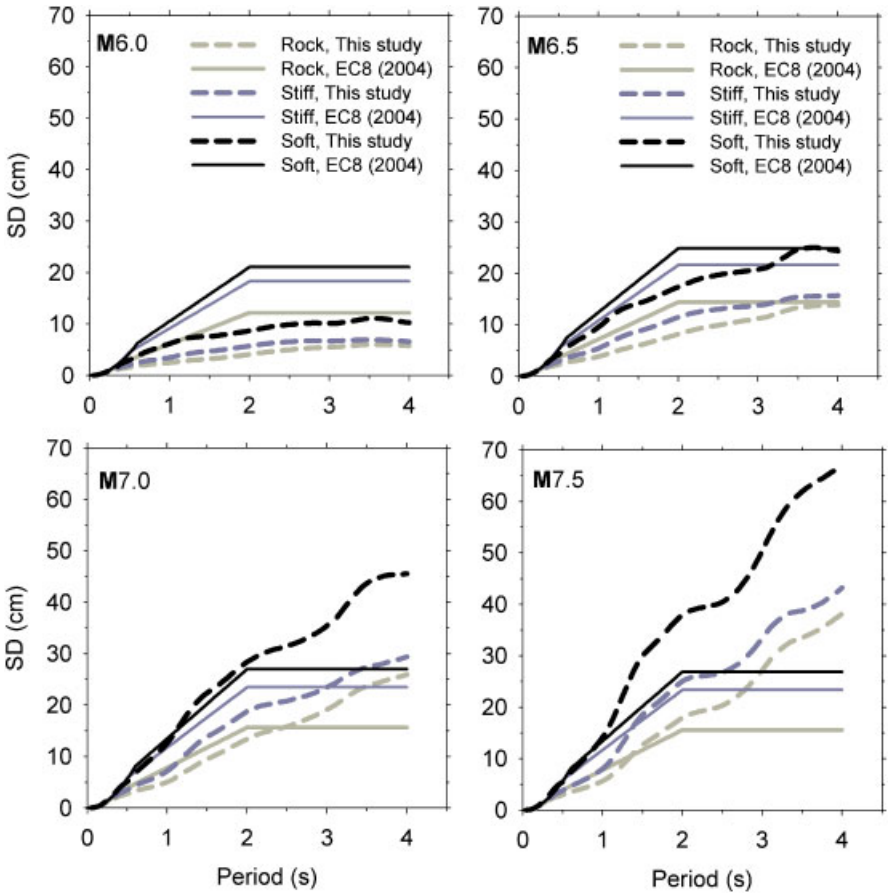

Figure 7. Comparison of Type 1 spectra from Eurocode 8 with predictions from this study for a source-to-site distance R_{jb} of 5 km.

- The control period defining the start of the constant displacement plateau needs to vary with earthquake magnitude; the choice of 2 s for the Type 1 spectrum is a gross underestimation leading to dangerously low spectral displacements at longer periods. By using three or more parameters to construct the spectrum, the variation of this corner period with magnitude can be captured.
- Consideration should be given to providing more sophisticated scaling factors to obtain the spectral ordinates at damping values other than 5% of critical, to reflect the influence of the ground-motion duration.

5. CONCLUSIONS

An important issue raised by this study is to find out the longest response period for which it is possible to obtain reliable estimates of the spectral ordinates from empirical data. In this study,

DOI: 10.1002/eqe

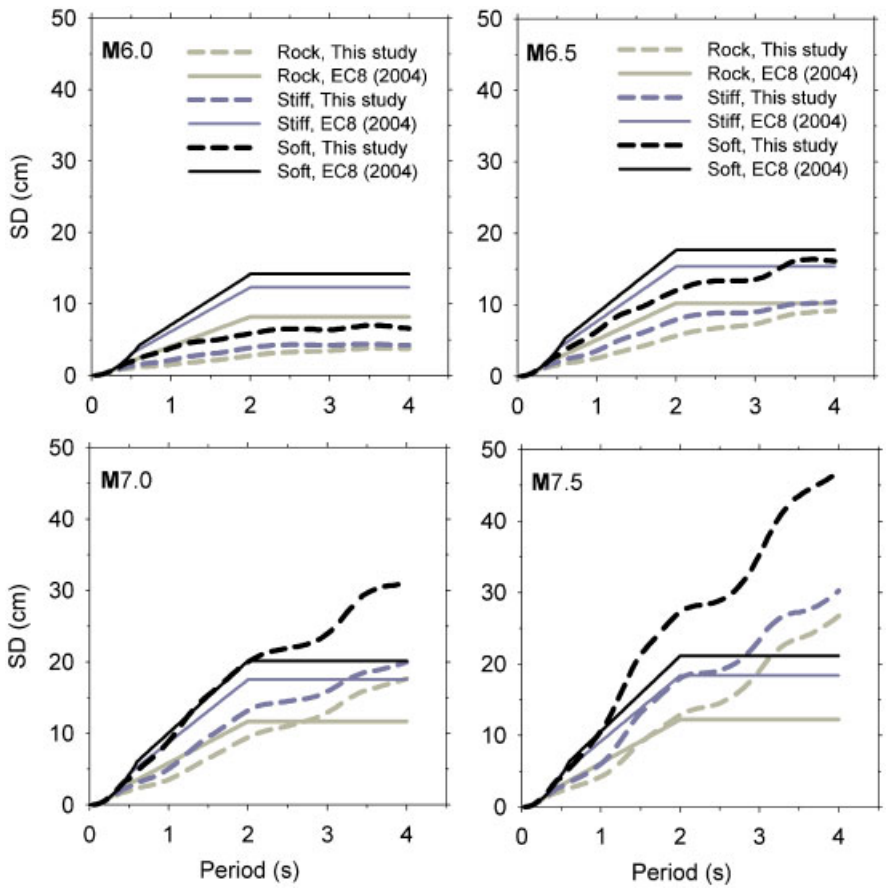

Figure 8. Comparison of Type 1 spectra from Eurocode 8 with predictions from this study for a source-to-site distance R_{jb} of 10 km.

we conclude that the limit currently attainable with the strong-motion data set from Europe and the Middle East is 4 s, although in the future, as the proportion of digital recordings grows, this can be expected to increase. However, applying the criteria established by Akkar and Bommer [21], even using only digital data, it is likely that reliable regressions could not have been obtained for a much longer period range. One possibility, recently much discussed but with few results published to date, is to use broad-band seismograms. Yu and Hu [27] use such data from southern California to derive empirical long-period spectral ordinate predictions, claiming that the data are reliable to periods as long as 20 s. In the Next Generation of Attenuation (NGA) project run by the Pacific Earthquake Engineering Research (PEER) Center, spectral ordinate predictions are being derived for periods up to 10 s [28], although some of the modellers so far seem to have limited their regressions to much shorter periods, such as Boore and Atkinson [29], who present equations only for periods up to 3 s. Campbell and Bozorgnia [30] present regression coefficients for periods

DOI: 10.1002/eqe

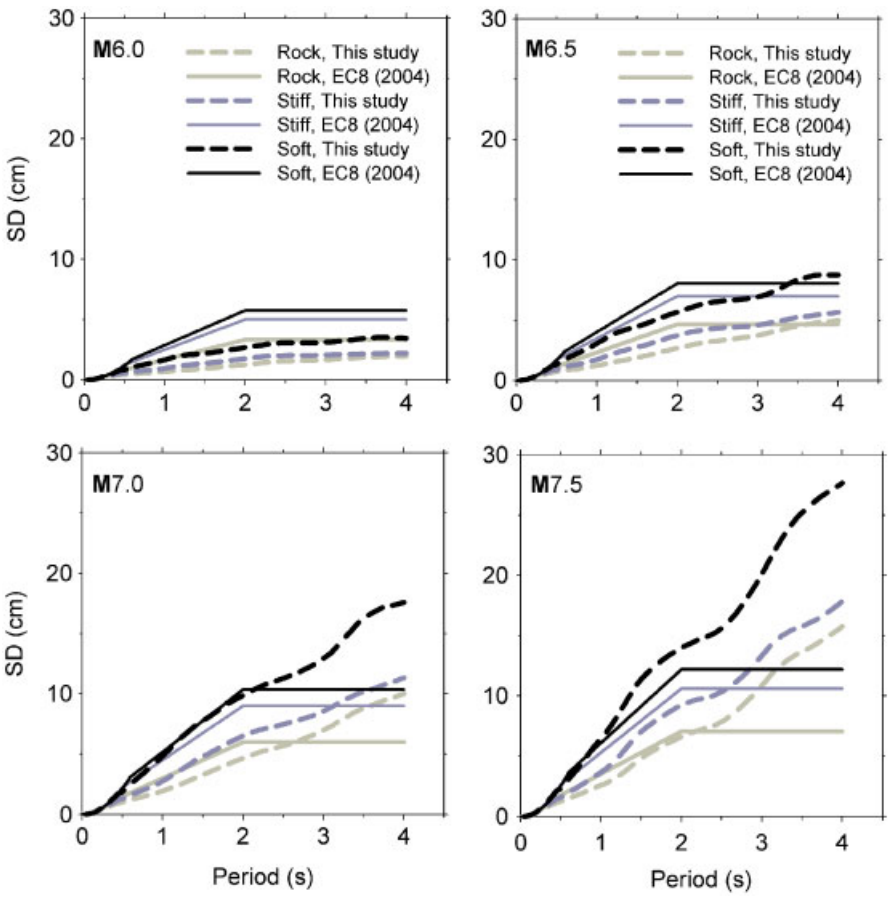

Figure 9. Comparison of Type 1 spectra from Eurocode 8 with predictions from this study for a source-to-site distance R_{jb} of 25 km.

up to 10 s, which are based purely on the empirical data. At 10 s period, only about one quarter of NGA data set can be used to derive spectral ordinates, for which reason some of the modellers in that project are also using seismological models to constrain the longer-period spectral ordinates (N.A. Abrahamson, personal communication, 2006).

The results confirm that the previous European displacement response predictions by Bommer *et al*. [23] are excessively low, particularly at longer periods. More significantly, perhaps, the results also show the spectral ordinates defined at intermediate- and long-periods in EC8 are severely underestimated as a result of the selection of a period of just 2 s for the start of the constant displacement plateau. In accordance with NEHRP 2003, this corner period, T_D, clearly is dependent on magnitude, but for events as large as **M**7 and greater, this control period lies beyond the 4 s limit of the equations presented herein. However, there is clearly a basis for modifying the definition of T_D in EC8 as a matter of urgency. This cannot be achieved as long as the EC8

DOI: 10.1002/eqe

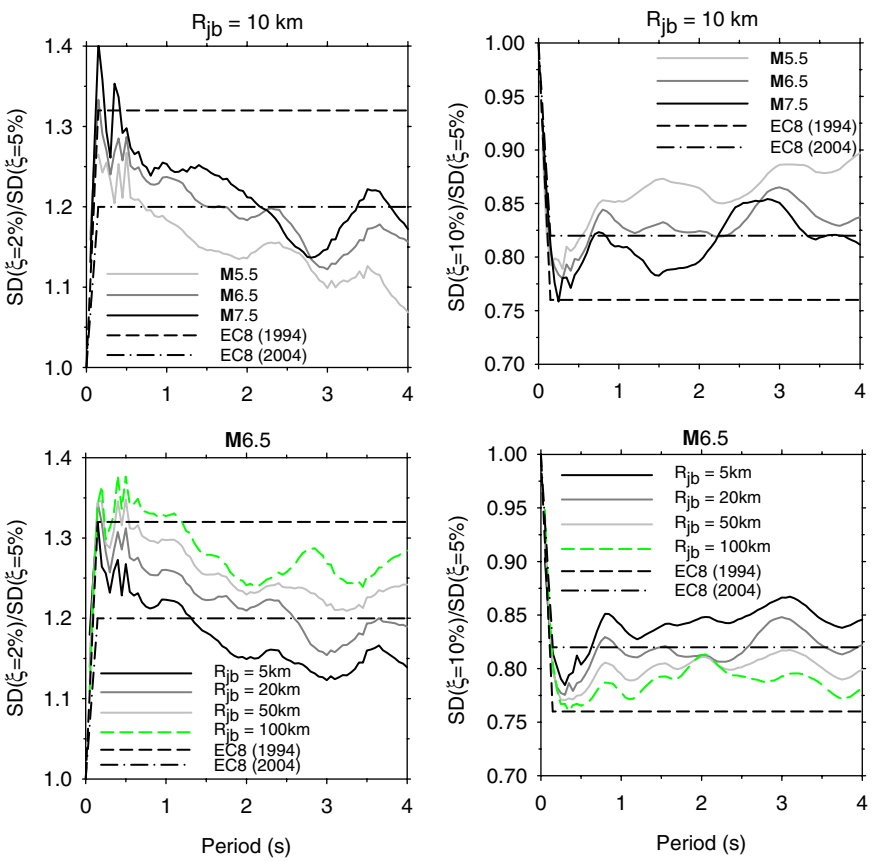

Figure 10. Spectral ratios with respect to the 5%-damped ordinates for 2% damping (left) and 10% damping (right) for different combinations of magnitude and distance.

spectrum is defined only in terms of PGA, and it is proposed that at least three parameters are considered for the construction of the displacement response spectrum in the code [5]. The new equations also indicate that whilst the current scaling factors in EC8 for damping values other than 5% of critical are a good general approximation (and an improvement to the factors in the original draft of EC8), the scaling shows a variation with magnitude and distance (reflecting the influence of duration) and also displays a mild dependence on the response period. Therefore, when a more elaborate procedure is adopted in the code for the construction of the displacement spectrum, these influences should also be accounted for as appropriate. The comparisons presented here are essentially deterministic but it would be useful to subsequently compare the EC8 spectra with uniform hazard spectra obtained from probabilistic seismic hazard analysis for a number of locations throughout Europe. Such comparisons are likely to confirm the findings of this study and strengthen the argument for moving away from the outdated procedure of constructing the elastic design spectrum anchored only to PGA.

DOI: 10.1002/eqe

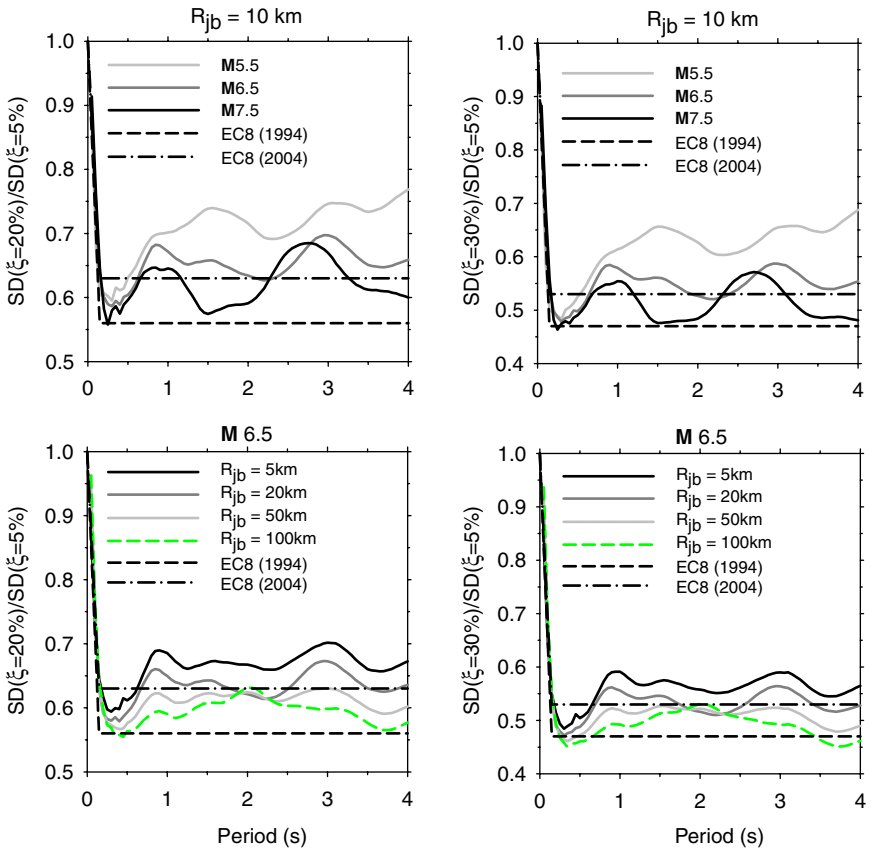

Figure 11. Spectral ratios with respect to the 5%-damped ordinates for 20% damping (left) and 30% damping (right) for different combinations of magnitude and distance.

ACKNOWLEDGEMENTS

The authors are grateful to John Douglas for his regression program and to John Alarcon for experimenting with the predictions from the new equations. The authors express their sincere gratitude to two anonymous reviewers for their constructive critiques during the review process.

REFERENCES

1. Kowalsky MJ, Priestley MJN, MacRae GA. Displacement-based design of RC bridge columns in seismic regions. *Earthquake Engineering and Structural Dynamics* 1995; **24**(12):1623–1643.
2. Akkar S, Miranda E. Statistical evaluation of approximate methods for estimating maximum deformation demands on existing structures. *Journal of Structural Engineering* (ASCE) 2005; **131**:160–172.
3. ATC. Improvement of nonlinear static seismic analysis procedures. *FEMA-440*, Applied Technology Council, CA, 2005.
4. CEN. *Eurocode 8*, *Design of Structures for Earthquake Resistance—Part 1*: *General Rules*, *Seismic Actions*, *and Rules for Buildings*, *EN 1998-1*:*2004*. Comité Européen de Normalisation, Brussels, 2004.

DOI: 10.1002/eqe

5. Bommer JJ, Pinho R. Adapting earthquake actions in Eurocode 8 for performance-based seismic design. *Earthquake Engineering and Structural Dynamics* 2006; **35**(1):39–55.
6. Boore DM. Long-period ground motions from digital acceleration recordings: a new era in engineering seismology. In *Directions in Strong Motion Instrumentation*, Gülkan P, Anderson JG (eds). Springer: The Netherlands, 2005.
7. FEMA. The 2003 NEHRP recommended provisions for new buildings and other structures. *Part 1*: *Provisions* (*FEMA 450*), Federal Emergency Management Agency, Washington, DC, 2003.
8. Boore DM, Bommer JJ. Processing of strong-motion accelerograms: needs, options and consequences. *Soil Dynamics and Earthquake Engineering* 2005; **25**(2):93–115.
9. Ambraseys NN, Simpson KA, Bommer JJ. The prediction of horizontal response spectra in Europe. *Earthquake Engineering and Structural Dynamics* 1996; **25**:371–400.
10. Ambraseys NN, Douglas J, Sarma SK, Smit P. Equations for the estimation of strong ground motions from shallow crustal earthquakes using data from Europe and the Middle East: horizontal peak ground acceleration and spectral acceleration. *Bulletin of Earthquake Engineering* 2005; **3**(1):1–53.
11. Berge-Thierry C, Cotton F, Scotti O, Griot-Pommera D-A, Fukushima Y. New empirical spectral attenuation laws for moderate European earthquakes. *Journal of Earthquake Engineering* 2003; **7**(2):193–222.
12. Tolis SV, Faccioli E. Displacement design spectra. *Journal of Earthquake Engineering* 1999; **3**(1):107–125.
13. Bommer JJ, Elnashai AS. Displacement spectra for seismic design. *Journal of Earthquake Engineering* 1999; **3**(1):1–32.
14. Faccioli E, Paolucci R, Rey J. Displacement spectra for long periods. *Earthquake Spectra* 2004; **20**(2):347–376.
15. Bommer JJ, Elnashai AS, Weir AG. Compatible acceleration and displacement spectra for seismic design codes. *Proceedings of the 12th World Conference on Earthquake Engineering*, paper no. 207. Auckland, 2000.
16. CEN. *Eurocode 8*, *Design Provisions for Earthquake Resistance of Structures*, *European Prestandard ENV 1998*. Comité Européen de Normalisation, Brussels, 1994.
17. Bommer JJ, Mendis R. Scaling of spectral displacement ordinates with damping ratios. *Earthquake Engineering and Structural Dynamics* 2005; **34**(2):145–165.
18. Mendis R, Bommer JJ. Constructing over-damped displacement spectra for seismic design codes. *Proceedings of the 8th US National Conference on Earthquake Engineering*, paper no. 1743. San Francisco, 2006.
19. Mendis R, Bommer JJ. Modification of the Eurocode 8 damping reduction factors for displacement spectra. *Proceedings of the 1st European Conference on Earthquake Engineering*, paper no. 1203. Geneva, 2006.
20. Akkar S, Bommer JJ. Empirical prediction equations for peak ground velocity derived from strong-motion records from Europe and the Middle East. *Bulletin of the Seismological Society of America* 2007; **97**(2).
21. Akkar S, Bommer JJ. Influence of long-period filter cut-off on elastic spectral displacements. *Earthquake Engineering and Structural Dynamics* 2006; **35**(9):1145–1165.
22. Makridakis S, Wheelwright SC, Hindman RJ. *Forecasting*: *Methods and Applications*. Wiley: New York, 1998.
23. Bommer JJ, Elnashai AS, Chilimintzas GO, Lee D. Review and development of response spectra for displacement-based design. *ESEE Research Report No. 98-3*, Imperial College, London, 1998.
24. Ambraseys NN, Free MW. Surface-wave magnitude calibration for European region earthquakes. *Journal of Earthquake Engineering* 1997; **1**(1):1–22.
25. Beyer K, Bommer JJ. Relationships between median values and between aleatory variabilities for different definitions of the horizontal component of motion. *Bulletin of the Seismological Society of America* 2006; **96**(4A):1512–1522.
26. Bommer JJ, Douglas J, Strasser FO. Style-of-faulting in ground-motion prediction equations. *Bulletin of Earthquake Engineering* 2003; **1**(2):171–203.
27. Yu Y, Hu Y. Empirical long-period response spectral attenuation relations based on southern California digital broad-band recordings. *Proceedings of the 13th World Conference on Earthquake Engineering*, paper no. 344. Vancouver, 2004.
28. Power M, Chiou B, Abrahamson N, Roblee C. The 'Next Generation of Ground Motion Attenuation Models' project: an overview. *Proceedings of the 8th US National Conference on Earthquake Engineering*, paper no. 2022. San Francisco, 2006.
29. Boore DM, Atkinson GM. Boore–Atkinson NGA empirical ground motion model for the average horizontal component of PGA, PGV and SA at spectral periods of 0.1, 0.2, 1, 2, and 3 seconds. *Interim Report for USGS Review*, 31 May 2006 (revised 6th July 2006).
30. Campbell KW, Bozorgnia Y. Campbell-Bozorgnia NGA empirical ground motion model for the average horizontal component of PGA, PGV and SA at selected spectral periods from 0.01–10.0 seconds. *Interim Report for USGS Review*, 31 May 2006.

DOI: 10.1002/eqe